

# Root Architecture and Mechanical Strength of Root-Soil Composites for Slope Protection: A Review

Jeevana Sasindu Wickramaarachchige<sup>1\*</sup>, Daim Safer Mughal<sup>2</sup>

<sup>1</sup>School of Environment and Civil Engineering, Chengdu University of Technology, Chengdu, China

<sup>2</sup>School of Management and Economics, Chongqing University of Post and Telecommunications, Chongqing, China

DOI: <https://dx.doi.org/10.51584/IJRIAS.2026.11013SP0021>

Received: 15 May 2026; Accepted: 20 May 2026; Published: 13 June 2026

## ABSTRACT

As extreme weather events driven by global climate change increasingly threaten slope stability, soil bioengineering has emerged as a highly sustainable alternative to traditional concrete retaining structures. However, accurately assessing the safety of vegetated slopes remains a significant engineering challenge. Early analytical frameworks, such as the widely used Wu-Waldron model, frequently overestimate slope shear strength by assuming all roots break simultaneously and by ignoring the complex spatial root architecture of root systems. This review critically examines the fundamental mechanics of root-soil composites, emphasizing the critical need to move beyond simple observations of plant presence toward precise architectural quantification. This study explores how essential structural metrics, particularly Root Length Density and Root Area Ratio, dictate the mechanical reinforcement of soil. The analysis details the size-dependent scaling of root tensile strength and the vital mechanical transition between brittle root breakage and ductile root pull-out a dynamic failure mechanism heavily influenced by changing soil moisture and interfacial friction. Furthermore, this study evaluates the necessary shift from classical limit-equilibrium models to more realistic progressive failure frameworks, such as the Fiber Bundle Model, alongside modern numerical approaches like Finite Element and Discrete Element modeling. Despite notable computational advances, significant knowledge gaps persist within the discipline. Specifically, there is a distinct lack of long-term data regarding root strength degradation following plant mortality, and researchers continue to face major logistical barriers when attempting non-destructive 3D imaging of root networks in the field. To address these limitations, this paper recommends implementing mixed-vegetation planting strategies that combine deep taproots for structural anchorage with dense, shallow fibrous roots for surface cohesion and then this study advocate for the integration of fully coupled thermo-hydro-mechanical-biological software models to accurately capture the progressive failure and environmentally sensitive nature of bio-engineered slope stabilization. Finally, this study evaluates the techno-economic life-cycle performance of nature-based solutions against conventional grey infrastructure, highlighting the critical need for long-term field validation programs to ensure climatic and edaphic generalizability.

**Keywords:** Soil bioengineering; Root architecture; Slope protection; Root-soil composite; Nature-based solutions.

## INTRODUCTION

The plant-soil-atmosphere continuum fundamentally governs the hydrological reinforcement of slopes, operating in tandem with mechanical stabilization. Roots extract subsurface water through transpiration, which directly increases matric suction and effective stress within the unsaturated soil zone, thereby delaying the onset of moisture-induced shallow landslides<sup>[1,2]</sup>. Fine root networks enhance localized water retention by creating abundant capillary pores, whereas vertical taproots can inadvertently form deep preferential flow channels<sup>[3]</sup>. Consequently, asymmetrical or highly concentrated root orientations can either dissipate or exacerbate localized zones of high pore-water pressure during severe storm events<sup>[1]</sup>. The hydrological benefits of vegetation display pronounced seasonal fluctuations, contributing significantly to slope stability during dry periods but diminishing

rapidly as soils approach saturation during prolonged rainfall, at which point mechanical reinforcement must bear the primary stabilizing load<sup>[4]</sup>.

Beyond hydrological regulation, the mechanical efficacy of root reinforcement is fundamentally dictated by the biochemical composition and microstructural properties of the plant tissues. Root tensile strength correlates directly with the inherent bio-polymer matrix, primarily comprising cellulose, hemicellulose, and lignin<sup>[1,5]</sup>. Cellulose acts as the main load-bearing component, with its polymer chains grouped into micro-fibrils that impart significant tensile resistance. Hemicellulose forms a stabilizing matrix and cross-linkages, while lignin provides rigid mechanical support and resists biodegradation. Furthermore, the geometric arrangement of these components, quantified as the micro-fibrillary angle, governs the delicate balance between root stiffness and ductility<sup>[1]</sup>. Empirical testing consistently demonstrates an inverse power-law relationship between root diameter and tensile strength; finer roots generally exhibit a higher concentration of tensile strength per unit area due to a lower incidence of structural defects and a higher proportion of young, resilient cortex tissues<sup>[1,6]</sup>.

Because individual roots within a composite soil mass possess varying diameters, lengths, and tensile strengths, they do not fracture simultaneously when subjected to an expanding shear zone. Advanced analytical methods, such as the Fiber Bundle Model, account for this progressive failure mechanism by distributing applied loads across intact roots and recalculating stress concentrations dynamically as the weakest roots rupture<sup>[1,7]</sup>. Even more sophisticated approaches, including the Root Bundle Model, incorporate a Weibull survival function to statistically capture the probability of progressive root failure based on normalized displacements and inherent material variability. By integrating strain-step loading and localized stress redistribution, these progressive failure models prevent the systematic overestimation of shear resistance that plagues simpler equilibrium calculations, offering a highly accurate reflection of post-peak softening and residual strength in vegetated slopes<sup>[8,9]</sup>.

The ultimate failure of a root-soil composite is not solely governed by root rupture, as the frictional interaction at the root-soil interface often dictates whether a root will snap or simply pull out of the soil matrix. Interfacial pull-out resistance is a system-level property mobilized by the relative displacement between the elongating root and the surrounding earth<sup>[10,11]</sup>. Fine roots are particularly susceptible to pull-out rather than breakage, undergoing a complex deformation process characterized by nonlinear elastic stretching followed by plastic yielding along the root length<sup>[11]</sup>. Root pull-out mechanics are highly sensitive to confining pressure, soil density, and moisture content; elevated soil moisture lubricates the root-soil interface, significantly reducing frictional resistance and promoting slippage long before the root's ultimate tensile capacity is reached<sup>[7,10,12]</sup>. To accurately capture these dynamics, modern constitutive models explicitly distinguish between the brittle failure threshold of root fracture and the strain-softening phase of complete root pull-out<sup>[10]</sup>.

The spatial orientation and inclination of roots relative to the principal stress direction exert a profound influence on the mobilization of available shear strength. Discrete element method simulations reveal that root arrangements oriented perpendicularly to the principal shear force chain such as those angled at 135 degrees relative to the horizontal plane, maximizing soil stabilization by ensuring the root network operates predominantly in tension. Conversely, roots aligned parallel to the shear direction provide minimal mechanical reinforcement, as internal forces increase only slightly through passive friction without activating the root's bending or tensile capacities. The architectural geometry of the entire root system also dictates large-scale failure modes; a grid-like or cross-distributed root arrangement effectively disperses shear energy and mitigates localized damage better than strictly vertical or horizontal configurations<sup>[13]</sup>. Plants with heart-shaped or complex branching topologies generate multi-directional tensile restraints that intercept potential slip surfaces more reliably than simple taproot structures<sup>[4,6]</sup>.

At the mesoscopic scale, root reinforcement fundamentally alters the microstructural arrangement and internal force transmission of the soil matrix. Homogenization theory and three-dimensional unit cell modeling demonstrate that penetrating roots reorganize force chains among discrete soil particles, transforming an isotropic soil mass into an orthotropic anisotropic composite<sup>[14,15]</sup>. When subjected to shear, the root-soil composite relies on interlocking and self-locking mechanisms, wherein soil particles become embedded within the microscopic grooves of the root epidermis<sup>[16,17]</sup>. This interlocking action physically constrains particle rotation and slippage, expanding the thickness of the shear band and transferring concentrated shear stresses into

tensile resistance within the root fibers<sup>[17,18]</sup>. A denser root network creates a highly connected force chain that distributes external loads evenly across a larger volume of soil, thereby preventing premature catastrophic collapse and increasing the overall ductility of the slope material<sup>[15,19]</sup>.

The mechanical integrity of vegetated slopes is continuously challenged by dynamic environmental stressors, including freeze-thaw cycles, dry-wet alternations, and seismic loading. Repeated freeze-thaw cycles degrade soil structure by inducing frost heave, increasing hydraulic conductivity, and reducing the cellulose and hemicellulose content within the roots, which directly diminishes their tensile strength<sup>[13]</sup>. However, the presence of an interwoven root network mitigates the severe loss of soil cohesion and restricts the development of freeze-thaw cracking on the slope surface. Under dynamic or cyclic seismic loading, roots serve as stabilizing anchors that reduce the soil's damping ratio and enhance its dynamic shear modulus, storing energy elastically and delaying structural degradation<sup>[18]</sup>. Furthermore, dry-wet cycles cause the repeated expansion and contraction of hydrophilic clay minerals, leading to cumulative microstructural damage; yet the biological cementation provided by root exudates acts to bind soil aggregates, preserving the mechanical properties of the composite against cyclical weathering<sup>[11,20]</sup>.

In complex geological environments, slope materials frequently consist of heterogeneous soil-rock mixtures rather than uniform fine-grained soils, introducing additional variables to root-soil interactions. Rock blocks within the soil matrix act as rigid skeletal components that guide root deviation, increasing root tortuosity and expanding the total root-soil contact area. The presence of stones alters the internal pore structure, transitioning connected pores into isolated voids as roots navigate around the rigid obstacles. This coupled root-soil-rock interaction creates a highly resilient composite structure where the roots bind the finer soil matrix while the rock blocks provide compressive resistance and interlock with the root network. Modifying conventional root reinforcement theories to incorporate a rock influence factor allows engineers to accurately calculate the equivalent cohesion of these ternary systems, optimizing the selection of herbaceous vegetation for gravelly or stony slopes<sup>[21]</sup>.

Translating these intricate micromechanical and biological phenomena into practical civil engineering design requires a departure from static, generalized assumptions. The long-term stability of bio-engineered slopes depends heavily on the temporal evolution of the root system, as root decay following plant death or timber harvesting causes a rapid and severe attenuation of tensile strength and a subsequent loss of soil reinforcement<sup>[22]</sup>. Vegetation selection must therefore balance initial rapid growth rates with the longevity and decay resistance of the root biomass<sup>[3]</sup>. Furthermore, optimal slope stabilization necessitates matching root architecture to specific soil stratigraphy and anticipated stress paths, recognizing that a combination of deep taproots for anchorage and dense fibrous roots for surface cohesion yields the highest overall factor of safety<sup>[5,23]</sup>. By integrating advanced three-dimensional modeling, mesoscopic contact mechanics, and dynamic environmental variables, engineers can precisely parameterize the mechanical contributions of living root systems to achieve sustainable and resilient infrastructure protection<sup>[15]</sup>.

## CHARACTERIZATION OF ROOT SYSTEM ARCHITECTURE

The categorization of root system architecture serves as a foundational element in understanding the biomechanical interactions between vegetation and soil. While traditional morphological frameworks broadly classify root systems into tap-like, heart-like, and plate-like structures based on their three-dimensional volumetric expansion, more nuanced topological systems are required to capture the exact geometric orientation of root branches<sup>[24-26]</sup>. To address this, Yen's classification system rigorously categorizes root architecture into H, M, R, V, and VH types based on specific branching patterns and directional growth<sup>[6]</sup>. Within this topological framework, the V-type architecture denotes a predominantly vertical taproot system with highly restricted horizontal lateral extension, primarily functioning as a deep structural anchor<sup>[27]</sup>. Conversely, the H-type represents a root network that expands almost exclusively within the horizontal plane, providing broad but shallow surface coverage<sup>[27]</sup>. The R-type architecture is characterized by a robust central root complemented by an abundance of oblique and vertical lateral branches, a configuration empirically proven to be highly effective at transmitting, distributing, and dissipating shear forces across a wide volume of the soil matrix<sup>[6,28]</sup>. The M-type architecture diverges by lacking a conspicuous main taproot, instead developing a highly branched, multidirectional network dominated by dense, fibrous roots that excel at binding shallow soil aggregates

together<sup>[27,28]</sup>. The VH-type serves as a transitional or balanced structural configuration, integrating both the deep vertical anchoring properties of the V-type and the lateral stabilizing spread of the H-type<sup>[6,27]</sup>. Recognizing these distinct architectural topologies is paramount for civil engineers, as the specific orientation of the roots relative to potential slip surfaces dictates whether the biological material will resist slope failure through tension, compression, or bending mechanics<sup>[6]</sup>.

To mathematically translate these complex biological architectures into variables suitable for geotechnical design, researchers rely heavily on precise quantitative metrics, most notably Root Length Density (RLD). RLD is defined as the cumulative length of all root segments per unit volume of the encompassing soil matrix, conventionally expressed in kilometers per cubic meter or centimeters per cubic centimeter<sup>[7,29]</sup>. The acquisition of accurate RLD data necessitates meticulous physical sampling, wherein undisturbed soil cores or carefully excavated soil blocks are gently washed to liberate the delicate root networks from adhering to soil particles without inducing structural damage<sup>[11,30]</sup>. The extracted roots are subsequently arranged on specialized transparent trays to prevent overlapping and are scanned using high-resolution optical devices<sup>[31]</sup>. Advanced image analysis software programs, such as WinRHIZO, are then employed to automatically process the digital images and calculate the total root length across various microscopic diameter classes<sup>[32,33]</sup>. From an engineering perspective, RLD is an exceptionally critical parameter because it comprehensively quantifies the extent to which a root system permeates and interweaves within the three-dimensional soil domain<sup>[29,30]</sup>. A highly elevated RLD indicates a dense, fibrous biological network capable of physically encapsulating soil aggregates, effectively restructuring the internal force chains of the earth mass, and providing superior, uniform resistance against localized shear deformation and water-induced surface erosion<sup>[29,30,34]</sup>.

While RLD provides a thorough volumetric assessment of root permeation, the Root Area Ratio (RAR) supplies a two-dimensional, cross-sectional metric that is absolutely indispensable for the mathematical formulation of civil engineering stability models. RAR is formally defined as the ratio of the total cross-sectional area of all roots intersecting a specific, potential failure plane to the total surface area of that defined soil plane<sup>[7,29,35]</sup>. Experimentally, determining RAR involves exposing a physical cross-section of the soil, either through field trenching or laboratory shearing, and precisely measuring the diameters of every individual root intersecting that specific geometric boundary using digital calipers or specialized void-analysis imaging techniques<sup>[10,29,36]</sup>. The cross-sectional areas of these individual roots are calculated, summed, and then divided by the total area of the reference plane to yield a dimensionless percentage<sup>[10,37]</sup>. RAR is universally utilized in geotechnical modeling because it serves as the primary biological input variable for classical limit-equilibrium frameworks, most prominently the Wu-Waldron Model (WWM) and progressive Fiber Bundle Models (FBM)<sup>[10,29,38,39]</sup>. In these analytical calculations, RAR is multiplied by the mobilized tensile strength of the plant roots to derive the apparent root cohesion, a supplementary mechanical parameter that is directly superimposed onto the soil's inherent cohesion within the standard Mohr-Coulomb failure criterion<sup>[39,40]</sup>. Consequently, the accurate measurement of RAR allows civil engineers to quantitatively predict the exact magnitude of mechanical reinforcement of a specific vegetation community will contribute to a precarious slope<sup>[10,37]</sup>.

The structural parameters of a root system are not strictly governed by genetics; they exhibit profound biological plasticity in direct response to localized physical soil constraints, particularly variations in soil dry density. As the dry density of a soil profile increases, the mechanical impedance against root elongation rises exponentially, while the concurrent reduction in macroscopic pore space severely restricts the oxygen circulation necessary for aerobic cellular respiration<sup>[30,41]</sup>. Consequently, vegetation growing in highly compacted soils typically exhibits a substantial decrease in total root length density and overall biomass accumulation<sup>[30,42]</sup>. To overcome this elevated mechanical resistance and continue foraging for resources, root systems adapt anatomically by increasing their average diameter, a biological response driven by the physical expansion of cortical cells and the pronounced thickening of xylem vessel walls. This structural remodeling significantly enhances the longitudinal stiffness and penetration capacity of the roots, although this mechanical adaptation inherently limits their spatial exploration and network connectivity<sup>[42]</sup>. Conversely, excessively loose soils characterized by very low dry densities also impede optimal root development; the lack of intimate root-soil contact restricts efficient water and nutrient absorption, leading to physiological nutrient stress and diminished root proliferation. Therefore, an optimal, intermediate soil density exists for any given species, balancing mechanical support with necessary porosity to maximize root biomass and subsequent soil reinforcement potential<sup>[30]</sup>. As shown in Figure

1, these biological responses demonstrate a clear inverse correlation between increasing soil dry density and root length density across varying planting configurations (R24, R48, R72). The sharp downward trajectory observed in denser configurations (R48, R72) from 1.3 to 1.6 Mg/m<sup>3</sup> highlights the severe restrictive impact of mechanical impedance on root expansion. Conversely, the localized peak at 1.4 Mg/m<sup>3</sup> for the R24 density empirically validates the existence of an optimal intermediate soil state that effectively balances mechanical support with necessary porosity.

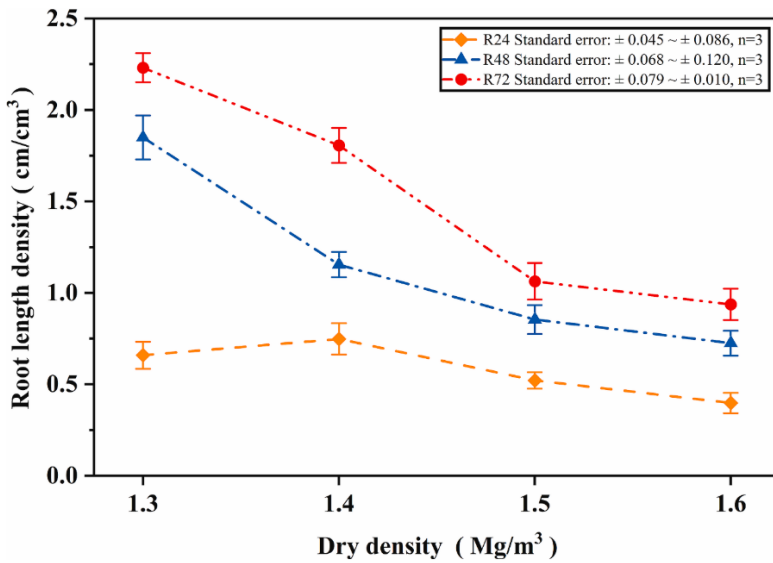


Figure 1: Effects of dry density and planting density on root length density<sup>[30]</sup>.

Soil moisture regimes exert an equally powerful influence on the biological plasticity, spatial distribution, and ultimate mechanical properties of plant root systems. In environments characterized by spatial moisture heterogeneity, roots demonstrate pronounced hydrotropism, actively extending their lateral architecture toward localized water-rich patches to sustain the plant's continuous transpiration demands<sup>[35,43]</sup>. Under conditions of moderate drought stress, many herbaceous species adapt by significantly increasing their specific root length, generating highly tortuous, fine roots that maximize the absorptive surface area per unit of carbon invested, thereby optimizing their foraging efficiency in arid conditions<sup>[44]</sup>. However, elevated soil moisture levels or prolonged flooding events fundamentally compromise both root architectural growth and inherent mechanical strength. Saturated conditions induce severe hypoxia within the soil pores, inhibiting cellular division and leading to a sharp decline in root length density, a reduction in active root tips, and eventually causing widespread tissue decay<sup>[45]</sup>. Furthermore, from a strict biomechanical standpoint, water acts as a potent plasticizer within the root's internal lignocellulosic matrix<sup>[46]</sup>. As the internal moisture content of the root tissues rises, the structural bonds between organic polymers in the cell wall weaken considerably, causing a drastic reduction in the root's ultimate tensile strength and increasing its susceptibility to mechanical failure under stress<sup>[46,47]</sup>.

The dynamic plasticity of root systems in response to fluctuating soil density and moisture carries profound implications for the design, execution, and long-term reliability of bio-engineered infrastructure. Because elevated soil moisture significantly diminishes intrinsic root tensile strength while simultaneously lubricating the root-soil interface, the predominant failure mechanism of vegetated slopes during intense rainfall events shifts critically from gradual root fracture to premature root pull-out<sup>[47-50]</sup>. This transition drastically curtails the mobilization of apparent root cohesion, meaning that a slope calculated to be perfectly stable under dry conditions may catastrophically fail upon saturation, despite the physical presence of a dense vegetation cover<sup>[47,49]</sup>. Furthermore, the radial expansion of coarse roots into the soil matrix physically compacts the adjacent rhizosphere, increasing the localized bulk density and altering the failure behavior of the composite earth from ductile strain-hardening to brittle strain-softening. This root-induced compaction can inadvertently create distinct localized planes of structural weakness that are highly susceptible to sudden shear failure under dynamic environmental loading<sup>[41]</sup>. Recognizing these intricate hydro-mechanical feedbacks, civil engineers cannot safely rely on static, homogenous values for root reinforcement; instead, sustainable slope stabilization

requires the integration of advanced constitutive models that explicitly account for dynamic spatial root distribution, specific architectural topologies, temporal tissue degradation, and the precise environmental stress thresholds of the selected plant species<sup>[10,22,47,51]</sup>. Figure 2 visually synthesizes these complex hydro-mechanical feedback and the overarching mechanisms of soil stabilization. Specifically, it highlights the dependence on the water content where excessive moisture lubricates the root-soil interface, reducing frictional resistance and promoting premature pull-out. Furthermore, the diagram illustrates how an overabundance of roots can inadvertently form preferential flow channels and localized structural weaknesses, reinforcing the critical need for dynamic, environmentally responsive constitutive models.

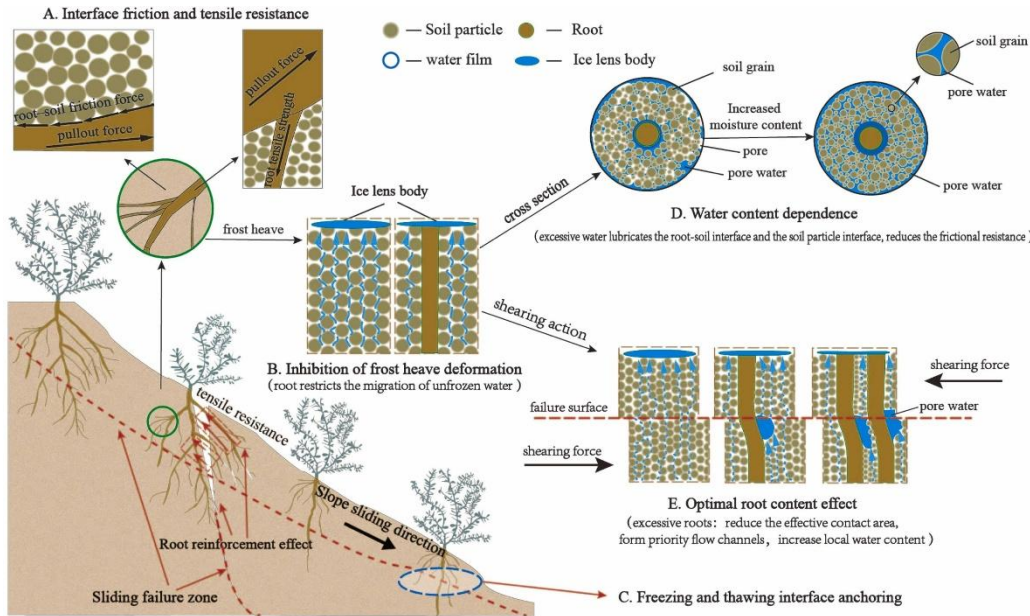


Figure 2: The influence mechanism of soil stabilization<sup>[49]</sup>.

## MECHANICAL PROPERTIES OF INDIVIDUAL ROOTS

The mechanical characterization of individual plant roots is a critical prerequisite for evaluating the stabilization of bio-engineered slopes, as the load-bearing capacity of a root-soil composite relies heavily on the mobilization of tensile resistance within the root system. When subjected to shear displacement, the earth matrix transfers destructive forces to the embedded roots via interfacial friction, effectively converting the soil's susceptibility to shear failure into a demand for root tensile strength. The fundamental metric for quantifying this biological reinforcement is the root tensile strength, which exhibits a highly non-linear, size-dependent scaling behavior. Extensive empirical testing consistently demonstrates an inverse power-law relationship between root tensile strength and root diameter, mathematically formulated as  $T_r = \alpha d^{-\beta}$ , where  $T_r$  is the ultimate tensile strength,  $d$  is the mean root diameter,  $\alpha$  is a species-specific empirical scaling coefficient representing intrinsic material strength, and  $\beta$  is a decay exponent dictating the rate of strength attenuation<sup>[46,52,53]</sup>.

This size-effect scaling occurs because root tissues are highly heterogeneous biostructures. Finer roots exhibit a substantially higher concentration of tensile strength per unit area because they possess fewer structural micro-defects and consist primarily of a dense central stele rich in load-bearing cellulose<sup>[1,6,54]</sup>. As root diameter increases, the anatomical cross-section becomes dominated by less-tensile secondary structures, heavily lignified xylem, and softer cortical tissues, which inherently dilutes the overall material efficiency<sup>[1,46,54]</sup>. Advanced uniaxial tensile testing on the isolated structural components of Alfalfa roots precisely isolates this phenomenon, revealing that the tensile strength of the central stele scales as  $\sigma_L^t = 37.60d_s^{-1.13}$ , whereas the outer cortex scales at a fraction of that capacity,  $\sigma_{co} = 2.42t_{co}^{-1.13}$  (S. Wang et al., 2024). Consequently, the overarching tensile behavior of intact roots varies significantly across different vegetation types. For instance, the empirical constants for *Cynodon dactylon* are recorded as  $\alpha = 15.81$  and  $\beta = 0.69$ , demonstrating a high baseline efficiency, whereas *Digitaria sanguinalis* and *Imperata cylindrica* scale with  $\alpha = 26.25$ ,  $\beta = 0.35$  and  $\alpha = 20.18$ ,  $\beta = 0.37$ , respectively<sup>[53]</sup>. In contrast, woody and tall herbaceous species often display steeper

attenuation rates, such as Bamboo grass ( $\alpha = 24.85, \beta = 1.46$ ) and Lemon grass ( $\alpha = 72.59, \beta = 0.83$ ) (Kumar, Nainegali, et al., 2025). Similar evaluations report ( $\alpha = 30.295$  and  $\beta = 1.33$  for *Trifolium repens* L.<sup>[36]</sup>,  $\alpha = 41.031$  and  $\beta = 1/447$  for *Artemisia sacrorum*<sup>[6]</sup>, and  $\alpha = 18.878$  and  $\beta = 1.12$  for *Chrysopogon zizanioides*<sup>[6]</sup>). These constants highlight that while average tensile capacities may hover around 17.6 MPa for live radiata pine or 43.52 MPa for *Caragana microphylla*<sup>[37,56]</sup>, actual engineering calculations must discretize root populations by diameter to prevent dangerous overestimations of structural capacity. Table 1 consolidates these species-specific biomechanical parameters, illustrating the profound variance in structural scaling across different root architectures. By quantifying the scaling coefficient ( $\alpha$ ) and decay exponent ( $\beta$ ) alongside the overall tensile strength range for various herbaceous and woody species, the data empirically underscores the necessity of utilizing discrete, diameter-dependent strength profiles rather than generalized averages in geotechnical modeling.

Table 1: Summary of Species-Specific Root Biomechanics and Structural Scaling Parameters

Plant Species	Root System Architecture Type	Root Tensile Strength (MPa)	Scaling Coefficient ( $\alpha$ )	Decay Exponent ( $\beta$ )	Source
<i>Indigofera amblyantha</i>	Taproot (Shrub)	15 to 45	44.023	1.4719	[57]
<i>Dendrocalamus strictus</i> (Bamboo grass)	R-type	110.14	24.85	-1.46	[55]
<i>Cymbopogon citratus</i> (Lemon grass)	M-type	212.25	72.59	-0.83	[55]
<i>Sorghum bicolor</i> (Sudan grass)	tap roots	0.85-1.8	0.39	-1.43	[29]
<i>Cynodon dactylon</i>	fibrous root networks	39.34 ± 11.35	15.81	-0.69	[53]
<i>Digitaria sanguinalis</i>	fibrous root networks	41.90 ± 5.85	26.25	-0.35	[53]

The internal stress-strain behavior of an individual root under axial loading deviates considerably from isotropic linear elasticity, reflecting its complex composite anatomy. During initial loading, the root undergoes a non-linear elastic stretching phase governed by an elastic modulus that also decays as a negative power function of diameter, such as  $E_L = 386.78d_s^{-1.13}$  for Alfalfa stele tissue<sup>[54]</sup>. As axial strain increases, the deformation transitions from an elastic regime to plastic yielding. The structural failure of the root is rarely a singular, instantaneous event; rather, it follows a progressive fracture mechanism dictated by the hierarchical arrangement of internal fiber bundles. Uniaxial tension curves frequently exhibit step-like stress drops prior to total failure. These fluctuations represent the sequential snapping of weaker peripheral fiber bundles within the periderm<sup>[58]</sup>. When an individual fiber ruptures, its specific load is instantaneously transferred and redistributed to the surviving, intact vascular bundles, temporarily restoring the force equilibrium until the critical tensile threshold of the central xylem is reached<sup>[37,58]</sup>. This progressive structural degradation absorbs substantial strain energy, contributing a high degree of ductility to the root before the ultimate peak tensile force is recorded and the specimen snaps entirely<sup>[58]</sup>.

However, the theoretical mobilization of a root's ultimate tensile strength is entirely contingent upon the mechanical competence of the root-soil interface. If the frictional interaction between the root epidermis and the surrounding soil matrix is insufficient, the root will simply slip or pull out rather than fracture, drastically curtailing the reinforced shear strength<sup>[10,22,59]</sup>. The physical physics of this interfacial bond are governed by three primary mechanisms: micro-morphological interlocking, biochemical adhesion, and matric suction<sup>[17,52]</sup>. Physically, roots do not possess perfectly smooth cylindrical geometries; their surfaces feature intricate ribbing, micro-grooves, and dense networks of fine root hairs<sup>[16,60]</sup>. Soil particles actively embed themselves within these

microscopic cavities, generating a profound mechanical “biting” or “self-locking” effect<sup>[17,60]</sup>. This physical meshing resists shear displacement far more effectively than standard Coulomb friction<sup>[60]</sup>. Concurrently, roots exude organic biochemicals, such as mucilage, which act as biological adhesives that bind adjacent soil aggregates directly to the root epidermis, enhancing local interfacial cohesion<sup>[32,52]</sup>. Furthermore, active plant transpiration extracts localized pore water, elevating the matric suction within the adjacent rhizosphere. This suction physically draws soil particles closer together, exponentially increasing the normal effective stress acting upon the root surface, thereby amplifying the available static friction<sup>[41,61]</sup>.

The mechanical integrity of this bond is highly sensitive to environmental boundary conditions, particularly moisture content and radial compaction. As roots grow and radially expand, they displace and compact the immediate surrounding soil, locally increasing dry bulk density. This root-induced compaction transitions the localized soil behavior from strain-hardening to a dense, dilative strain-softening state, elevating both the internal friction angle and the normal confinement acting on the root<sup>[41]</sup>. Conversely, elevated soil moisture critically compromises interface mechanics<sup>[49]</sup>. As saturation increases, matric suction rapidly dissipates, reducing effective normal stress<sup>[61]</sup>. The excess water hydrates and softens the biological exudates, creating a lubricating film at the interface that prevents the soil grains from interlocking with the root's micro-grooves<sup>[32,49]</sup>. Under these saturated conditions, the failure mechanism reliably shifts from a state of static self-locking to premature, ductile pull-out, long before the root's internal fibers can mobilize their full tensile capacity<sup>[22,49,59]</sup>. As shown in Figure 3, the pull-out mechanics of discrete roots follow a complex, multi-stage trajectory. The initial steep rise from point O to M reflects the simultaneous mobilization of static friction and elastic stretching. Once the critical debonding threshold is reached at peak M, the root enters a sliding phase (M-K) characterized by a non-linear decay in force due to the continuous reduction of the root-soil contact area. The final abrupt drop at point K signifies the ultimate mechanical failure or complete extraction of the root fiber from the earth matrix.

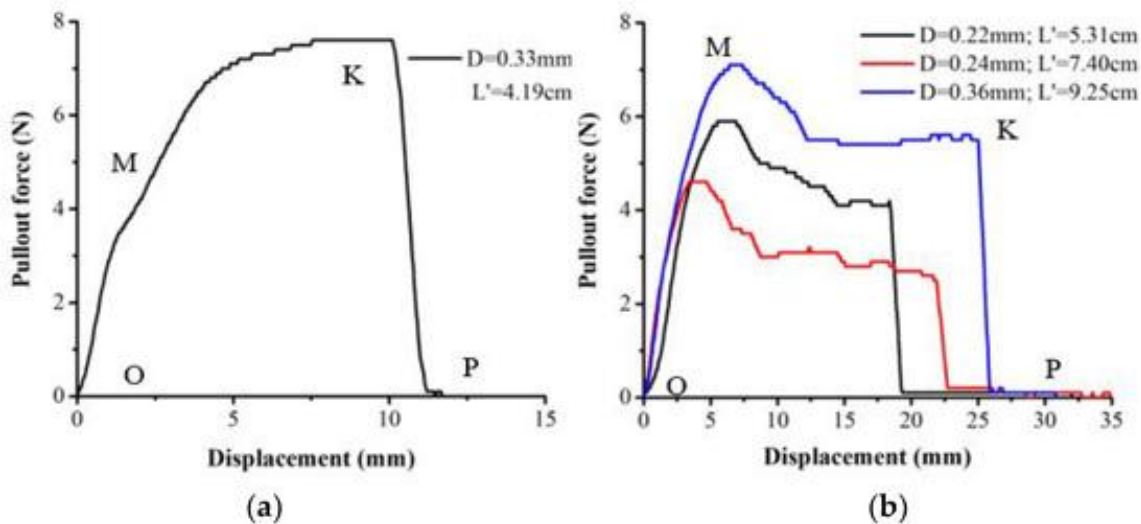


Figure 3: Force-displacement curves illustrating the mechanics of root pull-out<sup>[116]</sup>.

The mechanics of a discrete pull-out event represent a complex, multi-stage interaction characterized by dynamic stress redistribution along the root length. When a shear plane initiates within the soil, the intersecting root is subjected to localized transverse and axial loads<sup>[21,62]</sup>. Initially, the system behaves quasi-elastically; the segment of the root bridging the shear zone elongates, mobilizing static friction along its embedded length<sup>[63,64]</sup>. Because the root possesses inherent elasticity, the interfacial shear stress is not uniform; it peaks at the exact location of the slip surface and decays exponentially along the distal anchorage length<sup>[65]</sup>. As the applied force escalates, the shear stress near the fracture plane eventually exceeds the critical bonding strength of the soil-root interface. This initiates a progressive radial debonding phase<sup>[63,65]</sup>. Once deboned, the specific interface segment loses its static self-locking capability and transitions to dynamic sliding friction<sup>[17,63,65]</sup>.

This micromechanical transition dictates the macroscopic force-displacement response. Pull-out curves initially rise steeply as static friction and elastic stretching are mobilized simultaneously<sup>[6,66]</sup>. Once the critical debonding

threshold propagates along the entire embedded length, the root begins to physically translate out of the soil matrix. At this point, the load-displacement curve reaches its peak pull-out resistance. Following this peak, the system enters a distinct strain-softening phase<sup>[10,65]</sup>. The required pull-out force decays nonlinearly as the root slides out, driven by the continuous volumetric reduction of the root-soil contact area, which systematically diminishes the total available dynamic frictional resistance<sup>[10]</sup>. If the initial embedded length is sufficiently deep, and the confining pressure high enough, the cumulative static friction may exceed the ultimate tensile capacity of the root's central xylem, culminating in a sudden, brittle acoustic fracture characterized by an instantaneous drop in the load curve<sup>[10,22,67]</sup>. Ultimately, integrating these precise single-root failure dynamics, delineating exactly whether a specific diameter class will stretch, slip, or snap into continuum stability models is the only reliable method for accurately determining the safety factor of vegetated infrastructure under complex hydro-mechanical loading.

## MECHANICS OF ROOT-SOIL REINFORCEMENT

Root-permeated soil acts as a biological composite material where the earthen matrix supplies comprehensive compressive resistance and the embedded plant roots function as flexible, high-tensile structural fibers<sup>[10,68]</sup>. To mathematically evaluate the mechanical stability of these vegetated slopes, geotechnical engineers utilize an extended formulation of the classical Mohr-Coulomb failure criterion<sup>[1,7,69,70]</sup>. Within this limit equilibrium framework, the ultimate shear strength of the rooted soil is defined as the sum of the effective soil cohesion, the apparent cohesion provided by the root system, and the frictional resistance, which is dependent on normal stress and pore water pressure<sup>[1,2,40,70]</sup>. Extensive direct shear testing consistently demonstrates that while penetrating root networks can slightly alter internal force chains, their predominant mechanical contribution is a substantial increase in the cohesive intercept of the failure envelope<sup>[12,38,71]</sup>. The internal friction angle of the soil matrix remains largely unaffected or experiences only marginal modifications, primarily due to the generally random and heterogeneous spatial orientation of the complex root network<sup>[39,70-72]</sup>. Consequently, the mechanical reinforcement provided by vegetation is conventionally parameterized entirely through this additional apparent cohesion term, which is formally denoted in engineering literature as root cohesion, or  $c_r$ <sup>[38,39,70]</sup>.

The precise quantification of the parameter fundamentally relies on translating the biological and geometric traits of the root network into a singular, operational geotechnical variable. The most widely adopted analytical framework for this mathematical conversion is the perpendicular root reinforcement model, commonly referred to as the Wu-Waldron Model (WWM)<sup>[1,8,36,39]</sup>. The WWM calculates the apparent root cohesion as the direct product of the average mobilized root tensile strength, the root area ratio (RAR), and a geometric correction factor<sup>[1,26,36]</sup>. The root area ratio is defined as the total cross-sectional area of all plant roots intersecting a given shear plane divided by the total surface area of that specific soil plane<sup>[1,8,39]</sup>. The geometric correction factor explicitly accounts for the angular distortion of the roots as they stretch and deform across the expanding shear band; for typical internal friction angles and root distortion angles, this correction factor mathematically resolves to an empirical constant of approximately 1.2<sup>[1,2,36,40]</sup>. Despite its widespread engineering application, classical WWM operates under the highly idealized assumption that all roots possess identical elastic properties and will rupture simultaneously at the exact moment of slope failure<sup>[1,36,71]</sup>. This assumption systematically overestimates the actual tensile force mobilized by the composite system, necessitating the development of progressive failure frameworks, such as the Fiber Bundle Model, which explicitly accounts for the sequential snapping of roots and dynamic load redistribution based on distinct root diameter classes<sup>[1,10,36,37]</sup>.

The mechanical mobilization of this apparent cohesion relies entirely on a complex process of load transfer between the deforming soil matrix and the embedded biological fibers during a slope failure event. Prior to slope instability, plant roots remain in a relatively passive mechanical state<sup>[4]</sup>. However, as gravitational or hydrological forces induce active shear displacement along a potential sliding surface, the roots traversing this active shear zone are subjected to localized axial elongation and transverse bending<sup>[11,13,63]</sup>. The sliding soil matrix directly transfers these destructive shear forces into the root system via intense frictional and adhesive interactions mobilized at the root-soil interface<sup>[11,29,49]</sup>. The micro-morphological roughness of the root epidermis, combined with biochemical exudates and fine root hairs, physically interlocks with the surrounding soil aggregates, creating a profound mechanical bond<sup>[11,21,52]</sup>. Through this interfacial linkage, the applied shear stress is effectively converted into tensile stress within the lignocellulosic polymer chains of the root tissues<sup>[37,49]</sup>. This

critical stress transfer mechanism disperses localized shear energy across a significantly larger volumetric area of the soil profile, restricting relative particle rotation and preventing catastrophic slippage<sup>[11,15,18]</sup>. Consequently, the root-soil composite exhibits a highly ductile, strain-hardening behavior, requiring substantially greater shear displacement and strain energy to reach ultimate failure compared to unreinforced bare earth<sup>[10,37,73,74]</sup>.

The specific architectural topology of the plant root system strictly dictates the spatial distribution of this load transfer, producing two distinct yet highly synergistic stabilization mechanisms: deep anchoring and shallow reinforcement. The anchoring effect is predominantly provided by taproot systems, which are characterized by a massive, vertically oriented primary root that grows deeply into the underlying earth<sup>[7,25]</sup>. These coarse taproots function as rigid biological piles or dowels that penetrate directly through precarious, unconsolidated upper soil layers and firmly embed themselves into deeper, highly stable strata or weathered bedrock<sup>[1,18,75]</sup>. By intercepting these deep-seated potential slip surfaces, taproots provide immense axial pull-out resistance that directly opposes gravitational driving forces, mitigating massive block collapse and deep structural toppling<sup>[11,76]</sup>. Furthermore, the radial expansion of these thick taproots during their secondary growth phase physically compacts the adjacent rhizosphere, increasing the localized dry bulk density and generating elevated lateral confining pressures that further enhance the frictional resistance of the surrounding soil matrix<sup>[23,41]</sup>. While highly effective at preventing catastrophic structural failure, taproot systems inherently possess a relatively sparse distribution of lateral branches, severely limiting their ability to widely diffuse tensile stress across the broad horizontal expanse of the shallow soil profile<sup>[11]</sup>.

In direct contrast to the deep anchoring of vertical taproots, shallow lateral and fibrous root systems provide extensive mechanical reinforcement to the vulnerable surficial soil horizons. Fibrous root architectures consist of dense, highly branched networks of fine roots that expand horizontally and obliquely, thoroughly permeating the uppermost decimeters of the slope<sup>[7,73,75,77]</sup>. This extensive biological mesh creates a pronounced "surface mat effect" that tightly binds loose soil particles into highly cohesive, water-stable aggregates<sup>[7,11,23,28]</sup>. Fine roots demonstrate a pronounced size-effect scaling, possessing a significantly higher ultimate tensile strength per unit of cross-sectional area compared to coarse roots, primarily due to higher cellulose concentrations and fewer structural micro-defects in their young cortical tissues<sup>[1,78]</sup>. When subjected to external shear or tensile stress, such as the forces that generate tension cracks at the crest of a failing slope, this dense fibrous network physically bridges the developing fissures and heavily restricts lateral soil deformation<sup>[6,11,19]</sup>. The immense total surface area of a fibrous root system maximizes the available root-soil contact interface, generating unparalleled spatially distributed friction that intercepts shallow sliding planes with remarkable mechanical efficiency<sup>[11,79]</sup>.

The ultimate capacity of the root-soil composite to resist catastrophic shear failure is strictly governed by the localized failure modes of the individual roots bridging the active shear plane, which predictably manifest as either brittle breakage or ductile pull-out<sup>[17,22,80]</sup>. This micromechanical bifurcation is dictated by a strict force equilibrium between the intrinsic tensile strength of the root's vascular tissue and the maximum static frictional resistance mobilized along the root-soil interface<sup>[22,53]</sup>. If the interfacial bonding force generated by soil confinement and root epidermis friction exceeds the maximum load-bearing capacity of the root's internal cellulose fibers, the root will undergo rapid tensile fracture, absorbing maximum strain energy before abruptly snapping<sup>[17,22,67,80]</sup>. Conversely, if the external shear stress applied along the embedded root length overcomes the critical threshold of interfacial friction before the internal plant tissues reach their ultimate tensile limit, the root-soil bond will dynamically fail<sup>[22,53,63]</sup>. Following this complete interfacial debonding, the root transitions immediately into a strain-softening sliding phase, smoothly pulling out of the soil matrix while providing only residual dynamic frictional resistance<sup>[6,10,22]</sup>.

The physical manifestation of these two competing failure modes is highly dependent on both the root diameter and transient environmental conditions. Fine roots, characterized by a massive specific surface area and intimate encapsulation by fine clay particles, frequently develop interfacial bond strengths that far surpass their minute total tensile capacities, resulting almost exclusively in breakage failure under applied loads. Thick, coarse roots, however, possess immense internal tensile strengths but a lower surface-area-to-volume ratio, strongly predisposing them to overcome interfacial friction and cleanly pull out of the earth during a landslide event<sup>[11,17,22,53,66]</sup>. Furthermore, extreme variations in soil moisture exert a controlling influence on this precise mechanical threshold<sup>[7,12,62]</sup>. Under dry conditions, elevated matric suction physically compresses soil aggregates tightly against the root epidermis, exponentially increasing normal effective stress and actively promoting root

breakage. During intense rainfall infiltration, however, matric suction is rapidly obliterated, and the massive influx of moisture hydrates the biochemical mucilage at the root surface into a highly lubricating boundary layer<sup>[11,12,47]</sup>. This severe attenuation of interfacial friction dictates that roots will prematurely pull out rather than mobilize their peak tensile strength, causing a drastic, sudden reduction in the operational  $c_r$  value and triggering catastrophic flowslides even on densely vegetated infrastructure<sup>[7,53,59]</sup>.

## ECONOMICAL COST, MAINTENANCE & LIFE-CYCLE PERFORMANCE

The financial evaluation of slope stabilization assets reveals a severe divergence in both initial capital expenditures (CAPEX) and long-term operational expenditures (OPEX) between conventional grey infrastructure and bioengineered solutions. Traditional retaining walls, shotcrete revetments, and soil nailing systems demand exorbitant CAPEX driven by the necessity for heavy machinery, specialized construction expertise, and carbon-intensive manufactured materials<sup>[47,81,82]</sup>. In strict contrast, soil bioengineering offers drastic capital savings by substituting industrial materials with vegetative components. Cost-benefit analyses demonstrate that establishing vegetative covers, such as vetiver grass, generates initial cost savings ranging from 60% in Australian road shoulder applications to as high as 90% in Chinese slope stabilization projects<sup>[83]</sup>. In the United States, installing vetiver grass requires an initial investment of merely 10 to 30 USD per linear foot, with individual plant slips costing approximately 2 to 3 USD, eliminating the need for expensive structural earthworks<sup>[83,84]</sup>. Furthermore, the OPEX profiles of these two asset classes behave inversely over time. Grey infrastructure requires escalating operational budgets to fund routine structural inspections, crack sealing, and eventual concrete replacement as the structures weather<sup>[47]</sup>. Bioengineered slopes, however, experience front-loaded OPEX that drop to negligible levels once the living asset reaches maturity, resulting in substantially higher long-term internal rates of return<sup>[84]</sup>.

Asset management for bioengineered slopes requires a highly specific, two-phased maintenance strategy that contrasts sharply with the static upkeep of concrete structures. During the critical establishment phase spanning the initial months to the first two years bioengineered, slopes are highly vulnerable and require intensive, active maintenance<sup>[83,85]</sup>. Because the nascent root systems are shallow and incapable of accessing deep groundwater, artificial irrigation is mandatory; for instance, newly planted vetiver requires watering every ten days to prevent drought-induced mortality before maturity<sup>[84]</sup>. Concurrently with irrigation, systematic weeding is essential during this fragile period to eliminate interspecific competition, preventing invasive or undesirable plant species from hindering the growth and density of the engineered root network<sup>[7,86]</sup>. Once the vegetation transitions into the mature phase, the root-soil composite becomes self-sustaining, and maintenance demands decrease precipitously<sup>[84]</sup>. In this mature stage, operational interventions shift entirely toward structural canopy management. Engineers must employ scheduled cutting and pruning to limit the accumulation of above-ground biomass, which actively reduces unnecessary surcharge loads on the slope and minimizes the risk of wind-induced uprooting of larger vegetation<sup>[7,24]</sup>.

The fundamental life-cycle performance of vegetative and concrete stabilization systems progresses in opposite directions. Conventional grey infrastructure exhibits its maximum design strength on the day of construction completion. Over a typical design lifespan of 25 to 50 years, these rigid elements strictly degrade<sup>[87]</sup>. Exposure to cyclic temperature stress, biological aggression, continuous chemical carbonation, and the erosive impact of corrosive precipitation inevitably lead to mechanical fatigue, material cracking, and a permanent reduction in the structural safety factor<sup>[47,88]</sup>. Because concrete systems are inflexible, they cannot adapt to natural localized soil movements or differential settlement, frequently resulting in catastrophic shear fractures<sup>[81,89]</sup>. Conversely, bioengineered slopes operate as dynamic, self-reinforcing systems whose mechanical efficacy progressively improves over time<sup>[55]</sup>. As the vegetation develops, the continuous accumulation of root biomass expands the root area ratio and deepens the reinforced soil zone, steadily increasing the composite shear strength and apparent cohesion<sup>[20,25]</sup>. Unlike deteriorating rigid retaining walls, living root networks have the biological capacity to self-repair, continuously adapting to subsurface soil strains and providing resilient, long-term stabilization that scales with the lifespan of the ecological community<sup>[81]</sup>. The fundamental economic, operational, and mechanical differences between rigid grey infrastructure and dynamic soil bioengineering dictate their long-term asset viability. While concrete solutions offer immediate strength but strictly degrade over time, nature-based

solutions require early establishment upkeep but appreciate in structural and environmental value as they mature. This performance divergence across key lifecycle pillars is qualitatively synthesized in Table 2.

Table 2: Summary of techno-economic indicators, life-cycle performance, and environmental impacts of soil bioengineering relative to conventional grey infrastructure.

Evaluation Parameter	Soil Bioengineering (Nature-Based Solutions)	Conventional Grey Infrastructure (Concrete / Shotcrete)
Initial Capital Expenditure (CAPEX)	Low to Moderate	High
Establishment Phase Maintenance (Years 1–3)	High Demands	Negligible
Long-Term Operational Expenditure (OPEX) (Years 3+)	Low to Decreasing	High to Escaping
Temporal Strength & Performance Curve	Progressive Scaling	Progressive Degradation
Design Life-Cycle & Longevity	Indefinite	Finite (Typically 30–50 Years)
Primary Failure Mechanism Mode	Ductile and Progressive	Brittle and Sudden
Environmental Co-Benefits	High Value	Negative Impact

## ANALYTICAL AND NUMERICAL MODELING

To accurately quantify the mechanical reinforcement that plant roots impart to soil, geotechnical engineers have developed various mathematical and analytical models. The most widely adopted foundational framework is the Wu and Waldron Model (WWM)<sup>[9]</sup>. The WWM conceptualizes root reinforcement as an apparent root cohesion term added directly to the soil's inherent shear strength, operating under the extended Mohr-Coulomb failure criterion<sup>[26,90]</sup>. However, a major and frequently cited criticism of the WWM is its fundamental assumption that all roots traverse the shear plane perpendicularly and, critically, mobilize their peak tensile strength and fracture simultaneously upon soil failure<sup>[7,36]</sup>. In reality, root systems are highly heterogeneous, and roots fail progressively rather than instantaneously as shear strain increases<sup>[1,8]</sup>. Consequently, the WWM systematically overestimates the actual reinforcement capacity of the root network, sometimes predicting shear strengths up to 215% higher than measured in-situ values<sup>[9,37]</sup>. To mitigate this severe overestimation, engineers frequently apply an empirical correction factor to the WWM, typically ranging between 0.3 and 0.8, depending on the vegetation type and soil conditions<sup>[9]</sup>.

To address the inherent limitations of WWM, Pollen and Simon introduced the Fiber Bundle Model (FBM), which adapts composite material mechanics to simulate the progressive rupture of plant roots<sup>[1,8,36]</sup>. Unlike the simultaneous failure assumption of the WWM, the FBM explicitly accounts for the sequential breaking of individual roots; when the weakest root in the bundle reaches its specific tensile limit and snaps, the applied load is dynamically redistributed among the surviving intact roots<sup>[7–9]</sup>. If this newly redistributed stress exceeds the tensile capacity of another root, a cascading failure occurs until the entire structural bundle ruptures<sup>[9]</sup>. While the FBM offers a more realistic estimation of root cohesion than the WWM, traditional FBMs often rely on a global load-sharing assumption and presume that all roots fail exclusively through breakage rather than slipping out of the soil matrix<sup>[9,62]</sup>. To further refine this progressive failure approach, the Root Bundle Model (RBM) and its probabilistic extension incorporating a Weibull survival function (RBMw) were developed to explicitly distinguish between brittle root breakage and ductile root slippage, dynamically accounting for the variation in elastic properties across different root diameter classes<sup>[8,9,62]</sup>. As shown in Figure 4, classical analytical

frameworks like the Wu-Waldron Model (WWM) frequently lead to a “Predicted peak strength” (blue dashed line) that significantly exceeds the “Actual peak strength” (green line) measured during shear displacement. This discrepancy arises because the WWM assumes simultaneous root rupture, whereas the actual failure is a progressive process where roots mobilize strength at different strain levels. Furthermore, the figure 4 highlights the transition from the brittle post-peak softening of bare soil (red line) to the enhanced ductility and increased cohesive intercept provided by the root network.

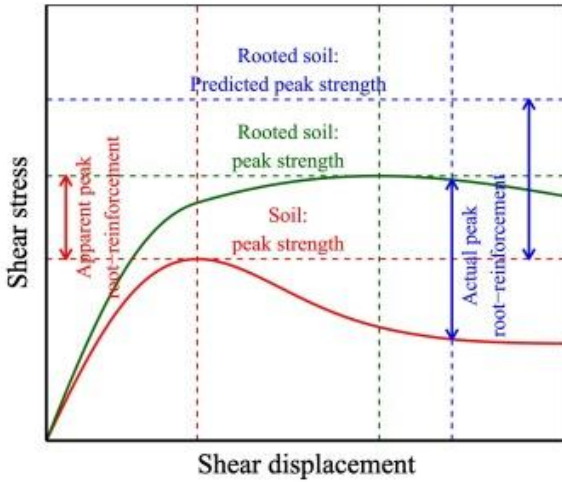


Figure 4: Comparison of predicted versus actual shear strength in root-reinforced soil<sup>[117]</sup>

While analytical limit-equilibrium models provide macroscopic apparent cohesion values, modern numerical methods attempt to simulate the exact spatial architecture and localized mechanical interactions of three-dimensional root systems. The Finite Element Method (FEM) is extensively utilized as a continuum-based approach that does not require a priori assumption of the critical slip surface's shape or location<sup>[70]</sup>. Within FEM frameworks, roots can be modeled either indirectly, by homogenizing the root zone and applying an apparent root cohesion factor, or directly, by embedding structural beam, pile, or cable elements into the continuous soil mesh to simulate flexural and tensile resistance<sup>[39]</sup>. Advanced FEM implementations utilize user-defined constitutive subroutines to model the coupled hydro-mechanical behavior of root-reinforced soils, tracking changes in matric suction and elastic-plastic deformation under complex stress paths<sup>[10,75]</sup>. Conversely, the Discrete Element Method (DEM) abandons the continuum assumption entirely, modeling the soil as an assemblage of individual rigid particles interacting via physical contact mechanics<sup>[13,91]</sup>. DEM is exceptionally suited for root-soil modeling because it visually and mathematically captures microscopic phenomena that FEM cannot easily resolve, such as the evolution of internal force chains, physical particle interlocking around root micro-structures, and the precise transitional mechanics from static interface friction to dynamic root pull-out<sup>[13,92]</sup>. By importing high-fidelity 3D root skeleton geometries which are often generated via algorithmic L-systems or 3D point-cloud scanning, into DEM software, engineers can evaluate specific architectural traits, such as root branching angles or asymmetrical morphologies, and alter localized shear band development<sup>[13,92,93]</sup>.

Despite the rapid advancement of these numerical techniques, translating the profound biological complexity of living root networks into reliable engineering software remains constrained by significant limitations. Primarily, the computational cost of simulating high-fidelity, three-dimensional root architectures using DEM or explicit smoothed particle finite element methods (eSPFEM) is exceedingly high, restricting these detailed microscopic analyses to small-scale unit cells or direct shear box dimensions rather than full-scale hillslope models<sup>[14,40,93]</sup>. Furthermore, accurately modeling the bidirectional feedback between biological growth and soil mechanics represents a major hurdle; as roots elongate and expand radially, they physically compact the surrounding rhizosphere, altering local porosity and mechanical impedance, yet most current simulations treat root geometry and soil density as static parameters<sup>[14,93]</sup>. Existing computational models also struggle to capture intricate biochemical and physiological variables at the mesoscopic scale, such as the exudation of mucilage that acts as a biological adhesive, the binding role of microscopic root hairs, and the rapid temporal degradation of root tensile strength due to organic decay following plant death or timber harvesting<sup>[22,41,52]</sup>. Additionally, the highly dynamic nature of the plant-soil-atmosphere continuum complicates hydro-mechanical coupling, as roots

constantly adapt their spatial distribution and transpiration rates in response to seasonal moisture fluctuations and localized drought stress<sup>[1,94]</sup>. Consequently, because natural root architecture is highly heterogeneous and governed by unpredictable environmental stressors, relying strictly on deterministic mathematical models without extensive site-specific experimental calibration often fails to capture the true, progressive failure mechanisms of vegetated infrastructure<sup>[57,62,94]</sup>.

## INFLUENCING FACTORS AND KNOWLEDGE GAPS

The mechanical efficacy of root-soil composites is not an isolated property; it is profoundly modulated by dynamic external environmental factors, most notably the hydrological regime and the resulting matric suction within the unsaturated vadose zone<sup>[1,95]</sup>. Through the physiological process of transpiration, vegetation continuously extracts soil moisture, which directly lowers the volumetric water content and induces a state of negative pore-water pressure, or matric suction<sup>[1,61]</sup>. This plant-induced suction alters the soil-water retention curve and acts as a supplementary confining stress that draws discrete soil particles closer together, thereby increasing the apparent cohesion and the overall shear strength of the earth mass<sup>[1,95,96]</sup>. However, this hydrological reinforcement is inherently transient and highly sensitive to external meteorological inputs. During periods of high-intensity or prolonged precipitation, the rapid infiltration of rainwater obliterates the matric suction, saturating the pore spaces and lubricating the root-soil interface<sup>[24,61]</sup>. As the soil transitions from an unsaturated to a fully saturated state, the critical threshold for interfacial friction diminishes, shifting the composite's failure mechanism from high-resistance root fracture to premature, low-resistance root pull-out<sup>[1,59]</sup>. Consequently, evaluating the performance of bio-engineered slopes requires a coupled hydro-mechanical approach that accounts for the continuous fluctuation of soil suction in response to extreme weather events and dynamic seasonal infiltration<sup>[1,57]</sup>. Table 3 summarizes the critical interactions between distinct root reinforcement mechanisms, their specific environmental sensitivities, and the corresponding analytical models used for evaluation. This matrix underscores the necessity of assessing bio-engineered slopes through coupled, environmentally responsive frameworks rather than isolated mechanical parameters.

Table 3: Interaction Matrix of Root Reinforcement Mechanisms, Environmental Sensitivities, and Analytical Framework

Root Reinforcement Mechanism	Influencing Environmental Factors	Analytical Models Used	Source
Soil binding / Aggregation	Mucilage secretion, Arbuscular mycorrhizal fungi (AMF) symbiosis, root hair length, rhizosphere biota	Penetrometer method, laboratory direct shear tests, Bivariate probabilistic modelling	[1]
Anchoring in stable soil layers	Soil moisture-related slope failure triggers (e.g., rain events)	W&W model, Fiber bundle model (FBM)	[7]
Tensile strength mobilization during root dragging	Soil foundation modulus (prevents root dragging)	Mathematical-analytical model (MAM), Hertz contact model	[63]
Mechanical anchorage and hydrological modification (root water uptake altering suction and moisture distribution)	Soil moisture distribution, suction levels under partially saturated conditions	Factor of safety (FOS) under seismic loading	[18]
Self-locking and interlocking mechanism	Water content (5%, 12%, 19%), rainfall-induced	Large-scale direct shear tests, 3D particle flow code (PFC3D) numerical analysis, 3D laser	[97]

based on micromechanical force chains	weakening, root type, root content ratio	scanning (fractal dimension of failure surface), Mohr-Coulomb criterion	
Deep anchoring vs. surface reinforcement	Post-felling root decay, timber removal, and climate-induced storm intensity	Back analysis on failed slopes, theoretical models of effects of timber harvesting	[70]
Tensile strength mobilization (root-soil interface friction and occlusion)	Soil water content, soil particle size, freeze-thaw cycles	Wu's model, Fiber bundle model	[16]

In tandem with environmental hydrology, the temporal dimension of vegetation, specifically the growth stage of the plants, exerts a controlling influence on the mechanical characteristics of the root-soil composite<sup>[20]</sup>. Unlike conventional synthetic reinforcement materials, living root systems are highly dynamic structures that continuously evolve in terms of biomass, morphological complexity, and material stiffness over their lifecycle<sup>[6,20]</sup>. During the early stages of plant establishment, the root network is typically sparse, fine, and shallow, providing minimal mechanical reinforcement or anchorage against shear stresses<sup>[85,94]</sup>. As the vegetation matures, the proliferation of higher-order lateral branches and the radial thickening of primary taproots significantly expand the root area ratio and the volumetric extent of the reinforced soil zone<sup>[20,36]</sup>. The accumulation of biochemical polymers such as cellulose and lignin within the maturing root tissues enhances their individual tensile strength and longitudinal stiffness, allowing the root system to absorb and dissipate greater magnitudes of strain energy during slope deformation<sup>[7,36]</sup>. Empirical triaxial and direct shear tests consistently demonstrate that the peak shear strength, internal friction angle, and apparent cohesion of root-permeated soils increase progressively with the plant's growth period, culminating when the vegetation reaches structural maturity<sup>[36,98,99]</sup>. However, this temporal reinforcement is not uniformly linear; it is subject to seasonal growth rhythms, intra-species competition, and localized environmental stressors, dictating that slope stability cannot be treated as a static parameter in geotechnical design<sup>[36,94]</sup>.

Transitioning from the active growth phase to the broader lifecycle of vegetation reveals one of the most critical and under-researched vulnerabilities in ecological engineering: the long-term durability of root reinforcement following plant death, disease, or timber harvesting. Current geotechnical paradigms frequently assume an idealized, continuous state of vegetative health, yet biological materials are inevitably subject to organic degradation<sup>[22]</sup>. Upon plant mortality, the cessation of physiological functions initiates a rapid microbial decomposition of the root biomass, preferentially consuming non-structural carbohydrates before degrading the load-bearing cellulose and lignin matrices<sup>[22,54]</sup>. This decay process precipitates a precipitous, exponential attenuation of root tensile strength and a complete loss of the interfacial bonding forces that previously mobilized shear resistance<sup>[22]</sup>. Furthermore, as the decomposing roots shrink and disintegrate, they leave behind continuous macroscopic voids and tubular cavities within the soil matrix<sup>[100]</sup>. These newly formed macropores transition from serving as structural reinforcement zones to acting as preferential flow pathways for subsurface water, drastically increasing soil hydraulic conductivity and exacerbating the risk of deep-seated moisture infiltration<sup>[22,100]</sup>. Despite the profound implications of this degradation, there is a conspicuous scarcity of long-term, longitudinal studies that systematically quantify the spatio-temporal kinetics of root decay across diverse species and varying soil biochemical environments<sup>[101]</sup>. The lack of comprehensive durability data prevents the accurate prediction of the "window of vulnerability", the critical period during which the decaying root system loses its mechanical competence before a replacement vegetation community can fully establish its own reinforcing network<sup>[56,94]</sup>. As shown in Figure 5, the mechanical competence of the root system undergoes a rapid decline immediately following plant death. The ultimate tensile force (a) shows a clear downward shift in the power-law relationship across all diameter classes as decay time increases from 0 to 90 days. This is further quantified by the exponential decay of tensile strength  $T_r$  (b), where finer roots ( $d < 1\text{mm}$ ) exhibit a steeper attenuation rate compared to coarser roots. This precipitous loss of strength highlights the "window of vulnerability" where the slope loses biological reinforcement before new vegetation can establish a replacement network.

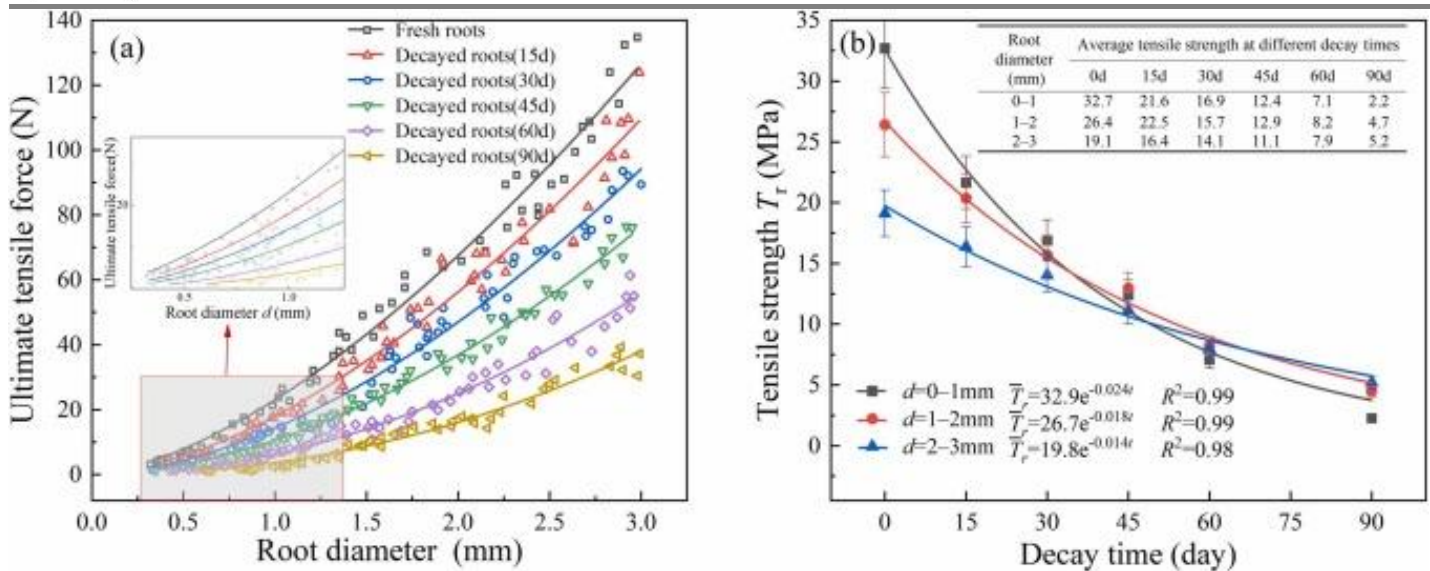


Figure 5: Temporal degradation of root mechanical properties following plant mortality<sup>[22]</sup>.

To accurately evaluate the stabilizing performance of root-soil composites and transition from theoretical limit-equilibrium calculations to real-world applications, geotechnical engineers must implement robust in-situ monitoring frameworks. Field validation fundamentally relies on the deployment of precision instrumentation to continuously capture the coupled hydro-mechanical responses of vegetated slopes<sup>[102]</sup>. The hydrological regime is meticulously tracked using time-domain reflectometry (TDR) sensors to measure volumetric water content, alongside high-sensitivity tensiometers and piezometers that record dynamic fluctuations in matric suction and positive pore-water pressure<sup>[94,102-104]</sup>. Simultaneously, the mechanical deformation and internal stress redistribution within the slope are captured using distributed fiber-optic strain sensors (DFOSS), in-place inclinometers, and tiltmeters<sup>[94,105]</sup>. For large-scale spatial assessments, these embedded sensor networks are increasingly augmented by terrestrial Light Detection and Ranging (LiDAR) and unmanned aerial vehicle (UAV) photogrammetry, which quantify surficial morphology, erosion progression, and macroscopic slope displacement without physical disturbing the fragile root-soil interface<sup>[84,94,105]</sup>. By centralizing data acquisition from these multi-tiered sensory arrays, researchers can establish empirical correlations between vegetation traits, atmospheric inputs, and the real-time structural integrity of the slope<sup>[102,106]</sup>.

The real-world accuracy of predictive slope stability models is profoundly challenged by the extreme spatiotemporal variability of climatic regimes and the inherent heterogeneity of regional geological conditions. In tropical monsoon and humid climates, high-intensity and prolonged precipitation events rapidly obliterate the transpiration-induced matric suction within the unsaturated zone, elevating pore-water pressure and systematically shifting the dominant failure mechanism from high-resistance root fracture to premature, ductile pull-out<sup>[94,102]</sup>. Conversely, in semi-arid environments or during prolonged seasonal droughts, the excessive evapotranspirative demand of vegetation can induce severe moisture deficits, precipitating the formation of deep desiccation cracks<sup>[1,84]</sup>. These tension fissures are particularly catastrophic in slopes composed of highly plastic expansive clays such as those found in the JiangHuai region of China or the southern United States, where cyclical shrink-swell behavior irrevocably degrades soil shear strength and provides preferential infiltration pathways for subsequent rainfall<sup>[84,107,108]</sup>. Furthermore, in highly erodible and collapsible geological formations, such as the wind-deposited loess of the Chinese Loess Plateau, the mechanical reinforcement of root networks is frequently counteracted by the soil's extreme sensitivity to localized moisture variations and freeze-thaw degradation<sup>[5,41]</sup>. Because current predictive models frequently homogenize these intricate hydro-mechanical boundary conditions, they regularly fail to capture the anisotropic flow patterns and dynamic stress responses dictated by specific localized weather extremes<sup>[94]</sup>.

Despite significant advancements in numerical and physical modeling, a critical research gap persists regarding the scarcity of comprehensive, multi-year field data capable of validating long-term slope performance. The vast majority of existing empirical literature is derived from small-scale laboratory direct shear or triaxial tests, which utilize remolded soils and severely restricted root architectures, thereby failing to replicate the complex boundary

conditions, root-induced compaction, and natural heterogeneity of field-scale hillslopes<sup>[25,41,101]</sup>. Moreover, these short-term laboratory studies inherently omit the temporal dimension of biological reinforcement, specifically the profound attenuation of tensile strength caused by seasonal dormancy and the progressive organic decay of roots following plant mortality or timber harvesting<sup>[46,56,94,101]</sup>. To effectively bridge the severe disjunction between controlled mesoscopic laboratory conditions and macroscopic hillslope realities, future research paradigms must prioritize the establishment of longitudinal, in-situ monitoring programs<sup>[101,109]</sup>. By continuously tracking the hydro-mechanical evolution of vegetated slopes across multiple climatic cycles, engineers can acquire the requisite datasets to calibrate advanced, fully coupled thermo-hydro-mechanical-biological (THMB) constitutive models<sup>[94,110]</sup>. This long-term empirical validation is absolutely essential for predicting the lifespan of bio-engineered infrastructure, optimizing species-specific planting strategies, and ensuring the sustainable mitigation of landslide hazards under an increasingly volatile global climate<sup>[9,94,101]</sup>.

The quantitative assessment of these complex architectural and temporal changes is further hindered by significant methodological limitations, particularly the profound difficulty of conducting non-destructive, three-dimensional imaging of root systems in the field<sup>[14,37]</sup>. In highly controlled laboratory settings, advanced techniques such as X-ray Computed Tomography (CT) and Magnetic Resonance Imaging (MRI) have revolutionized the mesoscopic study of root-soil composites, enabling researchers to precisely reconstruct intricate root topologies, observe progressive root-induced soil compaction, and perform detailed void analyses without physically disturbing the sample<sup>[14,73]</sup>. However, extrapolating these high-fidelity imaging technologies to in-situ field environments presents insurmountable logistical and technological barriers. The immense density of natural soil, the presence of heterogeneous rock inclusions, and the sheer spatial scale of mature tree root systems preclude the use of portable tomographic scanning<sup>[14,37,93]</sup>. Consequently, field-scale architectural quantification continues to rely heavily on highly destructive, labor-intensive methodologies, such as profile trenching, whole-plant excavation, and hydraulic washing<sup>[37,111]</sup>. These intrusive techniques irrevocably destroy the delicate micro-morphological interactions at the root-soil interface, obliterate the naturally occurring pore structures, and artificially alter the spatial orientation of fine roots<sup>[13,14]</sup>. This methodological bottleneck creates a severe disjunction between the idealized, static root geometries imported into numerical simulations and the actual, highly tortuous, and adaptive root architectures existing within natural slopes, thereby introducing significant uncertainty into the calibration of predictive stability models<sup>[14]</sup>. Table 4 presents a comparative evaluation of current root system characterization techniques, detailing their respective methodologies, advantages, and inherent limitations. This summary highlights the persistent technological bottleneck in the discipline, explicitly contrasting the high-resolution capabilities of laboratory-based non-destructive imaging with the destructive, labor-intensive realities of field sampling that continue to constrain accurate model calibration.

Table 4: Methodological Evaluation of Root System Characterization Techniques

Parameter / Technique	Measurement Methodology	Key Advantages	Inherent Methodological Limitations	Source
Advanced Non-destructive Imaging (X-ray CT)	Micro-focus industrial CT scanner (e.g., 160 kV, 50 μA) using "void analysis" and 3D reconstruction algorithms.	Enables non-destructive, high-resolution (voxel size ≈ 0.028 mm) observation of root development, 3D architecture, tortuosity, and spatial distribution within the soil matrix.	Small diameter fine roots (<0.25 mm) are often omitted; requires core soil extraction (small sample sizes); high computational power needed; herbaceous geometry remains largely unexplored.	[7,48,73]
Root Concentration (RLD/RD)	Manual excavation and washing of roots followed by WinRHIZO	Directly related to physical stability and shear strength; Root Density (RD) is	Labor-intensive; RD fails to distinguish between coarse and fine roots; significant bottleneck	[7,31]

	software analysis for length and biomass (dry weight).	relatively easy to obtain for fibrous systems.	between destructive field sampling and lab analysis.	
Root Tensile Strength	Single root tensile testing using clamp systems and servo-controlled machines (Force vs. Displacement).	Fundamental parameter for analytical models (Wu and Waldron Model (W&W) and Fiber Bundle Model (FBM)); captures species-specific mechanical reinforcement potential.	Time-consuming; measurement artifacts from clamp fixation often led to invalid results; inherent bias towards stronger roots.	[7,37]
Root-Reinforced Soil Stability	Constant Shear Drained (CSD) tests under saturated conditions mimicking rainfall infiltration scenarios.	Simulates static liquefaction and flowslide failure mechanisms more accurately than conventional triaxial tests.	Requires Skempton's B value calibration; potential for weak interfaces to cause volumetric dilation in long or stiff root samples.	[48]
Environmental Durability (Freezing/Thawing)	Frost heaving tests using upper/lower cooling plates followed by thawing in a direct shear box.	Simulates extreme environmental cycles to assess the durability of biological reinforcement under seasonal changes.	Laboratory simulation may not perfectly capture the complexity of infinite field soil boundaries or variable natural groundwater supply.	[73]
Surface-mat Effect	In-situ field pull-out tests and cantilever flexural strength analysis of interwoven topsoil plant fibers.	Redistributes local shear stress to stable sections; functions independently of soil moisture or texture failure triggers.	Concept is in its infancy; lack of standardized investigation and classification procedures.	[7,11]
Root System Characterization (General)	Qualitative assessment based on established relationships between measured root parameters and physical soil properties.	Circumvents time-consuming direct measurements of parameters like saturated hydraulic conductivity.	Severe technical bottleneck exists between destructive field sampling and advanced laboratory imaging techniques.	[30]

Despite significant advancements in soil bioengineering, current root-soil mechanics research remains constrained by pronounced geographic and taxonomic limitations. A substantial majority of empirical studies and modeling efforts are heavily clustered around specific, highly erodible geological environments, most notably the uniform, wind-deposited soils of the Loess Plateau or simplified sandy matrices while relying on a remarkably narrow selection of plant species<sup>[112,113]</sup>. Because the mechanical and hydrological interactions

between plant roots and the earth are intrinsically site-specific, generalizing these geographically concentrated findings to other ecological scenarios requires considerable caution<sup>[113]</sup>. Consequently, there is a critical need to expand experimental investigations into more diverse and problematic soil matrices that engineers frequently encounter in the field. This expansion must include highly weathered tropical laterite soils<sup>[114]</sup>, expansive clay soils that undergo severe volumetric shrink-swell deformation and extensive desiccation cracking<sup>[59,109]</sup>, and highly heterogeneous soil-rock mixtures where rigid stone inclusions fundamentally alter root growth trajectories, pore structures, and internal force chains<sup>[21]</sup>. To transition vegetation-based slope stabilization from a localized ecological practice into a universally applicable and standardized civil engineering solution, future research must establish comprehensive, regional vegetation-soil frameworks. By systematically validating predictive root reinforcement models across distinct climatic regimes spanning tropical, temperate, and arid environments practitioners will be able to develop standardized, climate-adaptive design guidelines that accurately pair specific plant functional traits with local geological demands<sup>[9,115]</sup>.

To resolve these pervasive regional, taxonomic, and methodological uncertainties and bridge the persistent divide between plant science and slope stability software, a fundamental paradigm shift is required in the development of constitutive geotechnical models. Historically, commercial slope stability software has accommodated vegetation merely by superimposing a static, homogeneous apparent cohesion value onto the classical Mohr-Coulomb failure criterion, a gross oversimplification that ignores the sophisticated biological realities of the plant-soil-atmosphere continuum<sup>[51]</sup>. Modern civil engineering software must evolve to integrate fully coupled thermo-hydro-mechanical-biological (THMB) frameworks that dynamically update soil parameters based on real-time plant physiological functions<sup>[57]</sup>. This integration necessitates the development of specialized subroutines such as those implemented via the Discrete Element Method (DEM) or advanced Finite Element Method (FEM) tools like ABAQUS and FLAC3D, that explicitly calculate the progressive, strain-dependent mobilization of root tensile strength rather than assuming simultaneous failure<sup>[52,57]</sup>. Furthermore, future computational models must import algorithms from functional-structural plant modeling (FSPM) to simulate the anisotropic growth of roots in response to soil mechanical impedance and localized moisture gradients<sup>[14]</sup>. By embedding biologically driven variables, such as root exudate-induced cementation, transpiration-driven matric suction transients, and species-specific decay kinetics, directly into the finite element mesh, software can accurately reflect the spatial heterogeneity and temporal volatility of vegetated slopes<sup>[57]</sup>.

Ultimately, advancing the discipline of ecological slope engineering demands a rigorous, interdisciplinary synthesis that transcends the traditional boundaries of botany, hydrology, and geotechnical engineering. The performance of root-soil composites is irrevocably tied to fluctuating external factors, from the microscopic capillary forces governing unsaturated soil suction to the macroscopic lifecycle stages of the overarching plant community<sup>[1,20]</sup>. Acknowledging and addressing the critical gaps in the current literature—namely, the dearth of empirical data on long-term root degradation, the narrow taxonomic and edaphic focus of existing field studies, and the technological barriers to non-destructive in-situ spatial characterization is essential for moving beyond empirical approximations<sup>[22,37]</sup>. By continuously refining coupled numerical algorithms that translate complex physiological plasticity into quantifiable mechanical feedback, researchers can develop predictive, climate-adaptive software tools that reliably assess slope resilience<sup>[14,94]</sup>. This integrated approach will not only enhance the accuracy of infrastructure safety assessments but also ensure the long-term ecological sustainability and mechanical viability of bio-engineered stabilization strategies in the face of escalating global climatic variability<sup>[94]</sup>.

## CONCLUSION

The mere biological presence of vegetation on a slope is fundamentally inadequate for determining geotechnical safety. Historically, assessing bio-engineered infrastructure relied on rudimentary observations of plant cover, treating root reinforcement as a static, homogeneous addition to soil cohesion that uniformly assumed simultaneous root rupture across a shear plane. However, true mechanical stabilization is dictated by precise architectural quantification, which mathematically translates the specific geometric and topological characteristics of a root network into operational engineering parameters. Quantifying traits such as Root Area Ratio, Root Length Density, spatial orientation, and diameter-dependent tensile strength allows engineers to accurately predict whether discrete root fibers will resist external loads through elastic tension, bending, or

interfacial pull-out. This critical distinction elevates bio-slope design from qualitative ecological observation to rigorous, verifiable geotechnical modeling that must be systematically expanded across diverse plant species, problematic soil matrices, and global climatic regions to ensure universal generalizability.

To effectively leverage these biomechanical mechanisms, civil engineers designing bio-slopes must implement multi-tiered, mixed-vegetation planting strategies rather than relying on monocultures. By strategically integrating deep-rooting woody species with shallow, fibrous-rooted herbaceous plants, designers can ensure that coarse taproots provide critical deep anchorage across deep-seated potential slip surfaces, while the dense fine-root networks mitigate surficial tension cracking and water-induced erosion. Additionally, engineers must abandon simplified, static limit-equilibrium calculations in favor of progressive failure frameworks and dynamic numerical simulations. Utilizing advanced computational tools, such as the Fiber Bundle Model or coupled hydro-mechanical finite element methods, ensures that design calculations explicitly account for the sequential fracture of varying root diameters, spatial heterogeneity, and the severe attenuation of tensile strength caused by elevated soil moisture and long-term root decay.

Ultimately, transitioning soil bioengineering into a standardized civil engineering paradigm requires moving beyond short-term laboratory boundaries to address real-world life-cycle performance and economic viability. Future research must prioritize long-term, multi-seasonal in-situ field monitoring programs to validate predictive hydro-mechanical models under highly volatile climatic and geological conditions. Furthermore, rigorous techno-economic assessments are critically needed to quantify the initial establishment maintenance demands, operational expenditures, and asset longevity of nature-based solutions in direct comparison to conventional concrete grey infrastructure. Only by reconciling these long-term operational, economic, and regional variables can ecological engineering provide a universally reliable, climate-adaptive alternative for sustainable infrastructure protection.

## REFERENCES

1. Bordoloi, S., & Ng, C. W. W. (2020). The effects of vegetation traits and their stability functions in bio-engineered slopes: A perspective review. In *Engineering Geology* (Vol. 275). Elsevier B.V. <https://doi.org/10.1016/j.enggeo.2020.105742>
2. Tsige, D., Senadheera, S., & Talema, A. (2020). Stability analysis of plant-root-reinforced shallow slopes along mountainous road corridors based on numerical modeling. *Geosciences* (Switzerland), 10(1). <https://doi.org/10.3390/geosciences10010019>
3. Yang, X., Chen, J., Dong, W., Liu, L., Wu, B., Xia, D., Liu, D., Zhao, B., Xu, Y., & Li, M. (2026). Root-mediated hydraulic performance of fibre-reinforced vegetation concrete (VC): The influence of root architecture, spatiotemporal evolution, and root vitality state. *Journal of Environmental Management*, 397. <https://doi.org/10.1016/j.jenvman.2025.128360>
4. Song, X., & Tan, Y. (2024). Experimental study on the stability of vegetated earthen slopes under intense rainfall. *Soil and Tillage Research*, 238. <https://doi.org/10.1016/j.still.2024.106028>
5. Cao, Y., Su, X., Zhou, Z., Liu, J., Chen, M., Wang, N., Zhu, B., Wang, P., & Liu, F. (2025). Effects of root traits on shear performance of root-soil complex and soil reinforcement in the Loess Plateau. *Soil and Tillage Research*, 252. <https://doi.org/10.1016/j.still.2025.106625>
6. Li, S., Wang, Z., & Stutz, H. H. (2023). State-of-the-art review on plant-based solutions for soil improvement. In *Biogeotechnics* (Vol. 1, Number 3). KeAi Communications Co. <https://doi.org/10.1016/j.bgtech.2023.100035>
7. Löbmann, M. T., Geitner, C., Wellstein, C., & Zerbe, S. (2020). The influence of herbaceous vegetation on slope stability – A review. In *Earth-Science Reviews* (Vol. 209). Elsevier B.V. <https://doi.org/10.1016/j.earscirev.2020.103328>
8. Arnone, E., Caracciolo, D., Noto, L. V., Preti, F., & Bras, R. L. (2016). Modeling the hydrological and mechanical effect of roots on shallow landslides. *Water Resources Research*, 52(11), 8590–8612. <https://doi.org/10.1002/2015WR018227>
9. DiBiagio, A., Capobianco, V., Oen, A., & Tallaksen, L. M. (2024). State-of-the-art: parametrization of hydrological and mechanical reinforcement effects of vegetation in slope stability models for shallow landslides. In *Landslides* (Vol. 21, Number 10, pp. 2417–2446).

Springer Science and Business Media Deutschland GmbH. <https://doi.org/10.1007/s10346-024-02300-1>

10. Liu, S., Ni, J., Zhao, X., Gao, Y., He, N., & Deng, Y. (2026). A new and simple hypoplastic model for saturated soils reinforced by plant roots. *Computers and Geotechnics*, 190. <https://doi.org/10.1016/j.compgeo.2025.107725>
11. Zhang, S., Ma, J., Liu, S., Zhang, L., Li, Z., She, F., Ding, J., Li, P., & Tian, C. (2025). Effects of herbaceous plant roots on tensile strength of root-soil composite in loess hilly region. *Catena*, 260. <https://doi.org/10.1016/j.catena.2025.109423>
12. Guo, P., Xia, Z., Liu, Q., Xiao, H., Gao, F., Zhang, L., Li, M., Yang, Y., & Xu, W. (2020). The mechanism of the plant roots' soil-reinforcement based on generalized equivalent confining pressure. *PeerJ*, 8. <https://doi.org/10.7717/peerj.10064>
13. Ni, J., Zhang, H., Liu, S., Deng, Y., & He, N. (2025). Experimental and DEM investigation of root orientation effects on shear behavior of soils subjected to freeze–thaw cycles. *Engineering Geology*, 359. <https://doi.org/10.1016/j.enggeo.2025.108433>
14. Zheng, H., Li, D., Wei, L., He, M., Sun, H., Zhu, L., & Xiao, M. (2026). Coupling root morphology and soil mechanics: The R–S MAFI model for predicting root–soil interactions. *Soil and Tillage Research*, 259. <https://doi.org/10.1016/j.still.2026.107092>
15. Huang, J. kun, Dai, J. pei, Scarpa, F., Wang, Y. qi, Ji, J. nan, & Mao, Z. (2025). Random root distribution affects the mechanical properties of the soil-root composite and root reinforcement. *Catena*, 255. <https://doi.org/10.1016/j.catena.2025.108896>
16. Sun, Y., Li, H., Cheng, Z., Dong, J., & Wang, Y. (2023). Experimental and Numerical Simulation Study on Mechanical Properties of Shallow Slope Root-soil Composite in Qinghai Area. *KSCE Journal of Civil Engineering*, 27(7), 2834–2852. <https://doi.org/10.1007/s12205-023-2366-0>
17. Gu, Q., Hong, B., Huang, Q., Kang, X., Zhang, D., Guo, X., Liu, G., & Xiao, T. (2025). Macro–Microscale Research on the Single Shear Characteristics of the Root–Loess Interface in Robinia pseudoacacia. *Agronomy*, 15(4). <https://doi.org/10.3390/agronomy15040847>
18. Shah, I., Jiang, Y. J., Alam, M., Xin, X., & Rehman, M. M. (2025). Sustainable slope stabilization: root-induced stiffness and damping control in sandy soils under cyclic loading. *Catena*, 261. <https://doi.org/10.1016/j.catena.2025.109576>
19. Huang, W., Tang, K., Lu, X., Yan, C., Yi, W., & Wang, M. (2026). Mechanical mechanism of MICP-reinforced irrigation-grass-root soil complex. *Results in Engineering*, 109153. <https://doi.org/10.1016/j.rineng.2026.109153>
20. Mao, Z., Wang, M., Xu, G., Geng, M., Ma, X., Gao, G., Tian, Y., Wang, L., & Xi, Y. (2025). The coupled temporal effects and micro-mechanism of root reinforcement and dry-wet cycles on the strength of herb-loess composite. *Soil and Tillage Research*, 253. <https://doi.org/10.1016/j.still.2025.106684>
21. Liu, J., Sun, S., Wei, J., Le, H., Cao, Y., Jin, C., & He, Y. (2026). Physical and mechanical properties of root-reinforced soil–rock mixture investigated by CT scanning and direct shear tests. *Catena*, 268. <https://doi.org/10.1016/j.catena.2026.110046>
22. Meng, S., Lu, S., Zhao, G., Hou, S., Lang, L., & Wang, S. (2026). Temporal evolution of mechanical properties of root-soil composites under plant root decay. *Soil and Tillage Research*, 257. <https://doi.org/10.1016/j.still.2025.106929>
23. Liu, F., Qi, S., Qi, S., Hou, X., Li, Y., Luo, G., Xue, L., Wang, X., Sun, J., Guo, S., & Zheng, B. (2024). In-situ Horizontal Extrusion Test of Herbaceous Root-Soil with Different Root Types. *Journal of Earth Science*, 35(3), 918–928. <https://doi.org/10.1007/s12583-022-1661-x>
24. Xue, L., Ding, H., Wang, H., Li, L., & Liu, H. (2024). Shallow slope stabilization by arbor root Systems: A physical model study. *Catena*, 246. <https://doi.org/10.1016/j.catena.2024.108458>
25. Ding, H., Xue, L., Liu, H., Li, L., Wang, H., & Zhai, M. (2022). Influence of Root Volume, Plant Spacing, and Planting Pattern of Tap-like Tree Root System on Slope Protection Effect. *Forests*, 13(11). <https://doi.org/10.3390/f13111925>
26. Temgoua, A. G. T., Kokutse, N. K., & Kavazović, Z. (2016). Influence of forest stands and root morphologies on hillslope stability. *Ecological Engineering*, 95, 622–634. <https://doi.org/10.1016/j.ecoleng.2016.06.073>

27. Lyu, S., Li, J., Lu, L., Ji, X., Liu, S., & Lyu, L. (2026). Enhancing soil deformation resistance in root-reinforced soils: quantitative analysis of root distribution patterns under cyclic traffic loading. *Acta Geotechnica*. <https://doi.org/10.1007/s11440-026-02978-8>
28. Jian, J., Su, W., Liu, Y., Wang, M., Chen, X., Wang, E., & Yan, J. (2024). Effects of Saline–Alkali Composite Stress on the Growth and Soil Fixation Capacity of Four Herbaceous Plants. *Agronomy*, 14(7). <https://doi.org/10.3390/agronomy14071556>
29. van den Broek, A. J., Mennes, D. T., Kleinhans, M. G., Roelofs, L., Eichel, J., Draebing, D., & de Haas, T. (2026). Impacts of plant roots on debris-flow bed erosion in laboratory experiments. *Engineering Geology*, 362. <https://doi.org/10.1016/j.enggeo.2025.108513>
30. Cui, L. X., Cheng, Q., So, P. S., Tang, C. S., Tian, B. G., & Li, C. Y. (2024). Relationship between root characteristics and saturated hydraulic conductivity in a grassed clayey soil. *Journal of Hydrology*, 645. <https://doi.org/10.1016/j.jhydrol.2024.132231>
31. Rong, Q., Yang, M., Deng, Y., Zhao, M., Liao, Y., Tan, Q., Pan, T., Yang, G., Yu, X., & Huang, Y. (2025). Influence of the root–soil complex on soil infiltration stages and their temporal changes in *Cunninghamia lanceolata* plantations. *Geoderma*, 464. <https://doi.org/10.1016/j.geoderma.2025.117606>
32. Cao, Y., Zhou, Z., Chen, M., Liu, J., Wang, P., Wang, N., Zhu, B., Liu, F., Wu, L., & Yu, D. (2026). Effects of gully topographic vertical zone on the spatial heterogeneity of root-soil complex shear performance in the loess plateau. *Catena*, 263. <https://doi.org/10.1016/j.catena.2025.109764>
33. Chen, Y., Ou, N., Ning, W., He, B., & Wang, G. (2026). Mechanisms controlling the inhibiting effects of roots on soil detachment through the growth of herbaceous plants in Southwest China. *International Soil and Water Conservation Research*. <https://doi.org/10.1016/j.iswcr.2026.100637>
34. Wang, J. F., Liu, G. Bin, Wang, B., & Ma, W. W. (2026). Root morphological characteristics as predominant factors enhancing soil resistance in typical grasslands of the Chinese Loess Plateau. *Soil and Tillage Research*, 261. <https://doi.org/10.1016/j.still.2026.107164>
35. Leblois, S., Calvani, G., Schwarz, M., Perona, P., Piton, G., & Evette, A. (2026). Willow root distribution on riverbanks for soil and water bioengineering design: From field measurements to soil reinforcement estimation. *Ecological Engineering*, 227, 107978. <https://doi.org/10.1016/j.ecoleng.2026.107978>
36. Jiang, B., Zhang, G., He, N., Li, X., Shi, C., & Xu, B. (2026). Reinforcement effect of *T. repens* L. influenced by soil depth, plant density and growth stage: experimental analysis and root cohesion models. *Results in Engineering*, 30. <https://doi.org/10.1016/j.rineng.2026.110273>
37. Hu, J., Wang, B., Bai, L., Li, Y., Zhang, X., Liu, J., & Zhao, C. (2024). Quantifying the contribution of shrub roots to soil mechanical reinforcement using in situ shearing and assessing model reliability in coal mine subsidence areas, China. *Catena*, 246. <https://doi.org/10.1016/j.catena.2024.108459>
38. Chirico, G. B., Borga, M., Tarolli, P., Rigon, R., & Preti, F. (2013). Role of Vegetation on Slope Stability under Transient Unsaturated Conditions. *Procedia Environmental Sciences*, 19, 932–941. <https://doi.org/10.1016/j.proenv.2013.06.103>
39. Dyson, A. P., Tolooiyan, A., & Griffiths, D. V. (2023). Numerical Modelling Techniques for Stability Analysis of Slopes Reinforced with Shallow Roots. *Geotechnics*, 3(2), 278–300. <https://doi.org/10.3390/geotechnics3020016>
40. Jia, X., Zhang, W., Wang, X., Jin, Y., & Cong, P. (2022). Numerical Analysis of an Explicit Smoothed Particle Finite Element Method on Shallow Vegetated Slope Stability with Different Root Architectures. *Sustainability (Switzerland)*, 14(18). <https://doi.org/10.3390/su141811272>
41. Li, R., Wang, H., Yan, Y., Han, C., Zhao, Y., Liu, Y., Shi, S., Ge, W., & Wang, F. (2025). Effects on soil structures by root growth in the Loess Plateau, China. *Catena*, 261. <https://doi.org/10.1016/j.catena.2025.109536>
42. Han, Q., Yang, Q., Guo, B., Colombi, T., Wang, J., Wu, H., Feng, Z., Zheng, Z., Li, Z., Zhang, Y., Han, M., Li, Q., Ding, J., Yang, X., Schneider, H. M., Zhao, Y., & Kong, D. (2025). Root structural remodeling under soil compaction for herbaceous plants. *Plant Diversity*. <https://doi.org/10.1016/j.pld.2025.12.008>

43. Zhang, J., Wang, J., Chen, J., Song, H., Li, S., Zhao, Y., Tao, J., & Liu, J. (2019). Soil moisture determines horizontal and vertical root extension in the perennial grass *Lolium perenne* L. Growing in karst soil. *Frontiers in Plant Science*, 10. <https://doi.org/10.3389/fpls.2019.00629>
44. Yang, Y., Chen, Z., Shi, H., Li, J., Wang, X., Gao, Y., Wang, P., & Wen, Z. (2026). Trait-based prediction of targeted species distributions facilitates environmentally adaptive vegetation restoration on the loess plateau. *Ecological Indicators*, 185. <https://doi.org/10.1016/j.ecolind.2026.114750>
45. Ju, Z., Fang, K., Wang, Y., Hu, B., Long, Y., Shi, Z., & Zhou, P. (2025). Effects of Flooding Duration on Plant Root Traits and Soil Erosion Resistance in Water-Level Fluctuation Zones: A Case Study from the Three Gorges Reservoir, China. *Water (Switzerland)*, 17(17). <https://doi.org/10.3390/w17172531>
46. Ji, K., Deng, C., Ye, L., Liu, Y., Liu, F., Mao, Z., & Zuo, J. (2025). Does Root Tensile Strength Exhibit Seasonal Variation? Evidence from Two Herbaceous Species. *Plants*, 14(19). <https://doi.org/10.3390/plants14192957>
47. Xue, L., Zhou, Y., Wang, H., Ding, H., Sun, Q., Li, L., & Huang, K. (2026). Impact of root diameter, length, and moisture content on the mechanical properties of root systems and the associated implications for ecological slope protection. *Catena*, 262. <https://doi.org/10.1016/j.catena.2025.109634>
48. Zou, X., Li, D., Wang, S., Gu, S., & Wu, W. (2024). Instability and deformation behaviors of root-reinforced soil under constant shear stress path. *Engineering Geology*, 343. <https://doi.org/10.1016/j.enggeo.2024.107762>
49. Zhang, M., Li, Q., Luo, X., Chen, W., Wang, R., Yu, S., & Yang, G. (2026). Effects of *Alhagi sparsifolia* root content and soil moisture content on soil deformation and strength under different freeze-thaw temperature conditions. *Soil and Tillage Research*, 260. <https://doi.org/10.1016/j.still.2026.107110>
50. He, L., Deng, Y. song, Tang, Q. yue, Liao, D. lan, Wang, C., & Duan, X. qian. (2022). Effects of the *Dicranopteris linearis* root system and initial moisture content on the soil disintegration characteristics of gully erosion. *Journal of Mountain Science*, 19(12), 3548–3567. <https://doi.org/10.1007/s11629-022-7448-9>
51. Wu, R., Wu, C., Xia, L., Long, G., & Ren, L. (2026). Active Earth Pressure in Unsaturated Retaining Walls Influenced by Vegetation Root. *Mathematics*, 14(6). <https://doi.org/10.3390/math14060995>
52. Xu, H., Wang, X. Y., Liu, C. N., Chen, J. N., & Zhang, C. (2021). A 3D root system morphological and mechanical model based on L-Systems and its application to estimate the shear strength of root-soil composites. *Soil and Tillage Research*, 212. <https://doi.org/10.1016/j.still.2021.105074>
53. Wang, R., & Liu, J. (2026). Root Tensile Functional Traits of Dominant Herbaceous Species and Their Effects on Soil Shear Strength in the Three Gorges Reservoir Drawdown Zone. *Applied Sciences (Switzerland)*, 16(5). <https://doi.org/10.3390/app16052333>
54. Wang, S., Liu, X., Qi, H., Xu, Z., & Ma, Y. (2024). Determination of Biomechanical Parameters and Development of an Improved FEM Model for Perennial Alfalfa (*Medicago sativa* L.) Roots. *Agronomy*, 14(12). <https://doi.org/10.3390/agronomy14123033>
55. Kumar, A., Nainegali, L., Das, S. K., & Reddy, K. R. (2025). Root reinforcement of herbaceous vegetation for stabilization of coal mine overburden dump slopes. *Bulletin of Engineering Geology and the Environment*, 84(12). <https://doi.org/10.1007/s10064-025-04640-1>
56. Watson, A., Phillips, C., & Marden, M. (1999). Root strength, growth, and rates of decay: root reinforcement changes of two tree species and their contribution to slope stability. In *Plant and Soil* (Vol. 217).
57. Badakhshan, E., & Vaunat, J. (2026). Thermo-hydro-mechanical modeling of root–soil interaction in unsaturated slopes. *Computers and Geotechnics*, 192, 107931. <https://doi.org/10.1016/j.compgeo.2026.107931>
58. Dai, X., xu, Z., Ye, H., & Zeng, Y. (2025). Triaxial test investigation of the reinforcement effect of *Acacia dealbata* roots on mountain red soil. *Scientific Reports*, 15(1). <https://doi.org/10.1038/s41598-025-27448-1>

59. Wang, G. Y., Huang, Y. G., Li, R. F., Chang, J. M., & Fu, J. L. (2020). Influence of vetiver root on strength of expansive soil-experimental study. *PLoS ONE*, 15(12 December). <https://doi.org/10.1371/journal.pone.0244818>
60. Tan, S., Xiang, G., Xu, X., & Liu, T. (2025). Mechanical characteristics of herbaceous plant root system and slope stability research. *Scientific Reports*, 15(1). <https://doi.org/10.1038/s41598-025-09581-z>
61. Wang, X., Liu, S., Lan, H., Sun, W., Ren, X., & Li, Z. (2025). Research of unsaturated strength characteristics for root–soil composite under different water content conditions. *Scientific Reports*, 15(1). <https://doi.org/10.1038/s41598-025-06444-5>
62. Fan, C. C., & Tsai, M. H. (2016). Spatial distribution of plant root forces in root-permeated soils subject to shear. *Soil and Tillage Research*, 156, 1–15. <https://doi.org/10.1016/j.still.2015.09.016>
63. Liu, X., Gao, P., Jiang, X., Guo, M., Wang, Y., & Ma, Y. (2025). Study on the interaction mechanism between stubble-breaking blades and unidirectional maize root-soil composites. *Biosystems Engineering*, 256. <https://doi.org/10.1016/j.biosystemseng.2025.104190>
64. Liu, X., Gao, P., Qi, H., Zhang, Q., Guo, M., & Ma, Y. (2024). Interaction Mechanisms between Blades and Maize Root–Soil Composites as Affected by Key Factors: An Experimental Analysis. *Agriculture (Switzerland)*, 14(7). <https://doi.org/10.3390/agriculture14071179>
65. Su, L. jun, Hu, B. li, Xie, Q. jun, Yu, F. wei, & Zhang, C. lei. (2020). Experimental and theoretical study of mechanical properties of root-soil interface for slope protection. *Journal of Mountain Science*, 17(11), 2784–2795. <https://doi.org/10.1007/s11629-020-6077-4>
66. Liu, J., Tang, Y., Pan, Y., Liu, Q., Wu, K., Xie, J., Xue, K., Liang, X., & Qi, L. (2026). Depth-dependent variations in shear strength of undisturbed root-soil composites of arbors: Insights from laboratory experiments on *Malus halliana* Koehne. *Bulletin of Engineering Geology and the Environment*, 85(3). <https://doi.org/10.1007/s10064-026-04842-1>
67. Kamath, A., van Bergen, K., Ravenshorst, G., & van de Kuilen, J. willem. (2025). Assessment of canal bank stability with vegetation root reinforcement. *Ecological Engineering*, 217. <https://doi.org/10.1016/j.ecoleng.2025.107623>
68. Waldron, L. J. (n.d.). The Shear Resistance of Root-Permeated Homogeneous and Stratified Soil 1.
69. Bordoni, M., Cislighi, & A., Vercesi, & A., Bischetti, G. B., & Meisina, & C. (n.d.). Effects of plant roots on soil shear strength and shallow landslide proneness in an area of northern Italian Apennines. <https://doi.org/10.1007/s10064-020-01783-1/Published>
70. Chok, Y. H., Jaksa, M. B., Kaggwa, W. S., & Griffiths, D. V. (2015). Assessing the influence of root reinforcement on slope stability by finite elements. *International Journal of Geo-Engineering*, 6(1). <https://doi.org/10.1186/s40703-015-0012-5>
71. Wang, R., Qin, C., Sun, H., & Feng, Y. (2024). Effects of root morphologies on shearing characteristics of the root-soil composite: An experimental case study of *Ficus virens* in Chongqing, China. *Catena*, 246. <https://doi.org/10.1016/j.catena.2024.108407>
72. Thouless, M. D. (2018). Shear forces, root rotations, phase angles and delamination of layered materials. *Engineering Fracture Mechanics*, 191, 153–167. <https://doi.org/10.1016/j.engfracmech.2018.01.033>
73. Song, B., Nakamura, D., Kawaguchi, T., Kawajiri, S., & Rui, D. (2025). Quantifying the shear behavior of fine-grained soil with herbaceous plant roots under freeze-thaw conditions using X-ray CT scan. *Soil and Tillage Research*, 246. <https://doi.org/10.1016/j.still.2024.106326>
74. Badhon, F. F., Islam, M. S., & Islam, M. A. (2021). Contribution of Vetiver Root on the Improvement of Slope Stability. *Indian Geotechnical Journal*, 51(4), 829–840. <https://doi.org/10.1007/s40098-021-00557-0>
75. Kang, X., Wang, S., Zou, X., Świtłała, B., & Wu, W. (2026). Hydro-mechanical response of herbaceous root-reinforced soils and its implications for vegetated-slope stability. *Engineering Geology*, 361. <https://doi.org/10.1016/j.enggeo.2025.108501>
76. Huang, R., Zhang, W., Xiang, J., Zhang, N., Oryem Ciantia, M., Yin, J., Liu, L., Wang, J., & Fei, A. (2026). Bearing capacity, shear band evolution, and deformation characteristics of slopes reinforced by root-inspired anchors using transparent soil model testing. *Journal of Rock*

- Mechanics and Geotechnical Engineering, 18(1), 457–471.  
<https://doi.org/10.1016/j.jrmge.2025.03.053>
77. Gribbe, S., Enderle, L., Coners, H., Hertel, D., & Leuschner, C. (2025). Fine root morphological traits and root dynamics of beech, oak, pine and Douglas fir along a climatic aridity gradient. *Plant and Soil*, 515(2), 2073–2099. <https://doi.org/10.1007/s11104-025-07706-x>
  78. Kunwar, B. B., Noppradit, P., Techato, K., & Gyawali, S. (2026). Floristic structure and root dynamics in slope stabilization of landslide-prone areas in the Phewa watershed, Nepal. *Journal of Mountain Science*. <https://doi.org/10.1007/s11629-025-9740-y>
  79. Liu, M., Luo, Y., Li, F., Hu, H., & Sun, D. (2023). Experimental Research on Erosion Characteristics of Ecological Slopes under the Scouring of Non-Directional Inflow. *Sustainability*, 15(20), 14688. <https://doi.org/10.3390/su152014688>
  80. Yu, L., Jing, T., Zhang, J., Xiao, H., & Zhou, L. (2025). Experimental study on synergistic reinforcement of riverbanks by enzyme-induced carbonate precipitation and plant roots. *Journal of Environmental Chemical Engineering*, 13(6). <https://doi.org/10.1016/j.jece.2025.119532>
  81. Thanasisathit, N., Chuenjaidee, S., Voottipruex, P., Jongpradist, P., Kalayasri, P., & Jamsawang, P. (2025). Field performance of erosion control on Lamtakong dam slopes using geocell and ruzi grass cover: A case study. *Geotextiles and Geomembranes*, 53(6), 1610–1622. <https://doi.org/10.1016/j.geotexmem.2025.08.010>
  82. Li, L., Liu, S., Gu, X., Liu, G., Zhang, X., & Xiong, H. (2026). Erosion control performance of natural geotextiles for slope stabilization. *Geotextiles and Geomembranes*, 54(1), 36–49. <https://doi.org/10.1016/j.geotexmem.2025.09.004>
  83. Kim, K., Riley, S., Fischer, E., & Khan, S. (2022). Greening Roadway Infrastructure with Vetiver Grass to Support Transportation Resilience. *CivilEng*, 3(1), 147–164. <https://doi.org/10.3390/civileng3010010>
  84. Rahman, F., Chakraborty, A., Khan, S., & Salunke, R. (2024). Impact of Vetiver Plantation on Unsaturated Soil Behavior and Stability of Highway Slope. *Geosciences (Switzerland)*, 14(5). <https://doi.org/10.3390/geosciences14050123>
  85. Liu, Z., Peng, Q., Yang, Q., Deng, H., Xiao, Y., Liu, D., & Yang, Y. (2026). Bio-geotechnical reinforcement of purple soil slopes: The synergistic effects of xanthan gum biopolymer and planting density. *Engineering Geology*, 362. <https://doi.org/10.1016/j.enggeo.2025.108540>
  86. Zhang, D., Cheng, J., Liu, Y., Zhang, H., Ma, L., Mei, X., & Sun, Y. (2018). Spatio-temporal dynamic architecture of living brush mattress: Root system and soil shear strength in riverbanks. *Forests*, 9(8). <https://doi.org/10.3390/f9080493>
  87. Nikolopoulos, D., & Makropoulos, C. (2026). The evolution of resilience from its ecological roots to critical infrastructure applications: Concepts, definitions and future directions. *International Journal of Critical Infrastructure Protection*, 53. <https://doi.org/10.1016/j.ijcip.2026.100848>
  88. Chatrabhuj, & Meshram, K. (2024). Use of geosynthetic materials as soil reinforcement: an alternative eco-friendly construction material. *Discover Civil Engineering*, 1(1). <https://doi.org/10.1007/s44290-024-00050-6>
  89. Wang, H., Zhang, R., Zheng, J., Song, X., Yang, T., & Wu, G. (2024). Numerical analysis of an enhanced flexible reinforcement system for expansive soil slopes based on on-site validation. *Bulletin of Engineering Geology and the Environment*, 83(8). <https://doi.org/10.1007/s10064-024-03833-4>
  90. Emadi-Tafti, M., Ataie-Ashtiani, B., & Hosseini, S. M. (2021). Integrated impacts of vegetation and soil type on slope stability: A case study of Kheyrud Forest, Iran. *Ecological Modelling*, 446. <https://doi.org/10.1016/j.ecolmodel.2021.109498>
  91. Tiwari, R. C., Bhandary, N. P., Yatabe, R., & Bhat, D. R. (2013). New numerical scheme in the finite-element method for evaluating the root-reinforcement effect on soil slope stability. *Geotechnique*, 63(2), 129–139. <https://doi.org/10.1680/geot.11.P.039>
  92. Zhang, L., Sun, J., & Shi, C. (2024). Numerical simulation on the influence of plant root morphology on shear strength in the sandy soil, Northwest China. *Journal of Arid Land*, 16(10), 1444–1462. <https://doi.org/10.1007/s40333-024-0030-2>
  93. Qin, K., Lu, J., Zhang, J., Cao, C., Huang, Z., Zhang, X., Gao, W., Zhu, X., Xue, K., Wang, L., Wu, Z., Bi, H., & Ge, J. (2026). Discrete element modeling and experimental validation of the

- multi-scale based coronal tea plant root-soil complex. *Computers and Electronics in Agriculture*, 245. <https://doi.org/10.1016/j.compag.2026.111585>
94. Kumar, A., Anand, A., Singh, R. V., Kumar, R., & Gohil, M. (2025). Vegetation hydrology and slope interaction under variable infiltration: a state-of-the-art review. *Journal of Infrastructure Preservation and Resilience*, 6(1). <https://doi.org/10.1186/s43065-025-00152-0>
  95. Wang, X., Wang, K. C., Deng, T., Wang, F., Zhao, Y. F., Li, J., Huang, Z., Wang, J. W., & Duan, W. H. (2024). Contribution of soil matric suction on slope stability under different vegetation types. *Journal of Soils and Sediments*, 24(2), 575–588. <https://doi.org/10.1007/s11368-023-03653-1>
  96. Ni, J., Liu, S., Huang, Y., & Gao, Y. (2024). Temperature and plant root effects on soil hydrological response and slope stability. *Computers and Geotechnics*, 174. <https://doi.org/10.1016/j.compgeo.2024.106663>
  97. Xu, Z., Ai, S., Sheng, M., Li, Z., Leng, Y., Ma, J., Zhu, G., & Ai, Y. (2025). Characteristics of carbon, nitrogen, and phosphorus in soil aggregates under different restoration methods on cut slopes in the Qinghai-Tibet Plateau mining area. *Journal of Environmental Management*, 393. <https://doi.org/10.1016/j.jenvman.2025.127166>
  98. Ma, X., Yu, Z., Liu, M., Wang, J., Su, Q., Zhang, J., Xie, J., & Wang, T. (2025). Mechanical properties and critical state characteristics of maize root-soil composites at different soil depths. *Biosystems Engineering*, 250, 163–173. <https://doi.org/10.1016/j.biosystemseng.2024.12.014>
  99. Ruihong, W., Kaiqiang, Z., Can, W., Xianda, Y., Kunpeng, L., & Dongbin, C. (2024). Slope protection effect of typical vegetation in the Three Gorges reservoir area under extreme rainfall. *IScience*, 27(6). <https://doi.org/10.1016/j.isci.2024.110057>
  100. Meng, S., Zhang, T., Zhao, G., & Hou, S. (2025). Time-varying mechanisms of hydraulic properties of root-soil composites under plant root decay. *Journal of Hydrology*, 658. <https://doi.org/10.1016/j.jhydrol.2025.133192>
  101. Munirwan, R. P., Milasafarah, S., Sungkar, M., Gunawan, H., Jaya, R. P., Taib, A. M., Yuliana, Y., & Kamchoom, V. (2025). Effectiveness of elephant grass roots in improving soil shear strength for slope reinforcement. *Results in Engineering*, 27. <https://doi.org/10.1016/j.rineng.2025.106369>
  102. Niyomukiza, J. B., & Eisazadeh, A. (2026). Hydro-Mechanical Performance of Vegetated Porous Concrete in Tropical Soils under Rainfall-Induced Slope Instability. *Biogeotechnics*, 100228. <https://doi.org/10.1016/j.bgtech.2026.100228>
  103. Mojid, M. A., & Cho, H. (2004). Evaluation of the time-domain reflectometry (TDR)-measured composite dielectric constant of root-mixed soils for estimating soil-water content and root density. *Journal of Hydrology*, 295(1–4), 263–275. <https://doi.org/10.1016/j.jhydrol.2004.03.012>
  104. Ma, S., He, B., Huang, Z., Ma, M., Wu, H., & Hu, Y. (2026). Field performance of a waterproof anchored vegetation system for protecting expansive soil slopes during rainy season. *Results in Engineering*, 29. <https://doi.org/10.1016/j.rineng.2025.108853>
  105. Liu, X., L&#xcfc;, X., Shao, Y., Chen, C., Liu, G., Li, Y., Li, M., Wu, X., & Chen, Y. (2024). Monitoring and disaster prevention of high and steep sandstone slopes along highways under construction. *Frontiers in Earth Science*, 12. <https://doi.org/10.3389/feart.2024.1444592>
  106. Huang, Z., Peng, Z., Jiao, W., Liu, Y., Xu, Y., & Ma, S. (2024). Field study on vegetation eco-protection technology for red sandstone fill slope against water damage. *Case Studies in Construction Materials*, 20. <https://doi.org/10.1016/j.cscm.2024.e03311>
  107. Huang, Z., Liang, Y., Xu, Y., Tang, H., & Jiao, W. (2025). Study on the protection of expansive soil slope by composite ecological lattice anchoring system under rainfall. *Case Studies in Construction Materials*, 22. <https://doi.org/10.1016/j.cscm.2025.e04604>
  108. Tao, W., Wen, Y., Bian, X., Ren, Z., Xu, L., Wang, F., & Zheng, H. (2024). Analysis of ecological prevention and control technology for expansive soil slope. *Frontiers in Earth Science*, 12. <https://doi.org/10.3389/feart.2024.1453178>
  109. Jiang, M., Lu, C., Wang, M., Mei, G., & Garg, A. (2026). Synergistic effects of drip irrigation and vegetation on the stability of biochar-stabilized expansive soil slopes. *Catena*, 264. <https://doi.org/10.1016/j.catena.2025.109761>
  110. Wei, L., Liang, S., Shan, X., Duojie, D., Liu, Y., Zhu, H., Li, G., & Hu, X. (2026). Soil infiltration and slope stability of shrub-covered loess slopes on the northeastern Qinghai–Tibet Plateau:

- experimental and numerical simulation. *Journal of Mountain Science*.  
<https://doi.org/10.1007/s11629-025-9954-z>
111. Rummel, P. S., Rasmussen, M. R., Saghaï, A., Merl, T., Hallin, S., Mueller, C. W., & Koren, K. (2026). Maize root growth, oxygen and N availability drive formation of N<sub>2</sub>O hotspots in soil. *Geoderma*, 467, 117734. <https://doi.org/10.1016/j.geoderma.2026.117734>
112. Bai, R., Zhao, X., Wang, X., Lv, W., Li, J., Yang, F., Shangguan, Z., & Deng, L. (2026). SOC erosion reduction of the “Grain for green” program on the Loess Plateau, China. *Soil and Tillage Research*, 256. <https://doi.org/10.1016/j.still.2025.106863>
113. Chen, Q., Yang, X. guo, & Zhou, J. wen. (2024). Assessing the mechanical effects of vegetation on the stability of slopes with different geometries and soil types. *Bulletin of Engineering Geology and the Environment*, 83(1). <https://doi.org/10.1007/s10064-023-03504-w>
114. Niyomukiza, J. B., Eisazadeh, A., & Tangtermsirikul, S. (2025). Influence of Bermuda Vegetation Roots on the Shear Strength Parameters of Laterite Soil. *Lecture Notes in Civil Engineering*, 677 LNCE, 490–497. [https://doi.org/10.1007/978-981-96-8464-9\\_62](https://doi.org/10.1007/978-981-96-8464-9_62)
115. Li, J., Li, L., Wang, Z., Zhang, C., Wang, Y., Wang, W., Zhang, G., Huang, J., Li, H., Lv, X., Pu, J., & Liu, J. (2021). The contributions of the roots, stems, and leaves of three grass species to water erosion reduction on spoil heaps. *Journal of Hydrology*, 603. <https://doi.org/10.1016/j.jhydrol.2021.127003>
116. Zhang, C., Feng, X., Qu, G., Yang, Q., & Jiang, J. (2023). How Does Embedding Angle Affect Root–Soil Mechanical Interactions? *Sustainability (Switzerland)*, 15(4). <https://doi.org/10.3390/su15043709>
117. Meijer, G. J., Knappett, J. A., Bengough, A. G., Bull, D. J., Liang, T., & Muir Wood, D. (2022). DRAM: A three-dimensional analytical model for the mobilisation of root reinforcement in direct shear conditions. *Ecological Engineering*, 179. <https://doi.org/10.1016/j.ecoleng.2022.106621>